Publicación Electrónica
ASOCIACIÓN PALEONTOLÓGICA ARGENTINA

www.peapaleontologica.org.ar

Cranial osteology and taxonomy of *Pronothrotherium* (Xenarthra, Folivora, Nothrotheriidae) from the late Miocene–early Pliocene of Catamarca Province (Argentina)

TIMOTHY J. GAUDIN[1]
SUSAN TUCKNISS[1]
ALBERTO BOSCAINI[2]
FRANÇOIS PUJOS[3]
GERARDO DE IULIIS[4]

1. Department of Biology, Geology and Environmental Science (Department 2653), University of Tennessee at Chattanooga. 615 McCallie Avenue, Chattanooga, TN 37403-2598, USA.
2. División Paleontología Vertebrados, Museo de La Plata, Unidades de Investigación Anexo Museo. Facultad de Ciencias Naturales y Museo, Calle 60 y 122, 1900 La Plata, Argentina; and, Instituto de Ecología, Genética y Evolución de Buenos Aires (IEGEBA – CONICET). DEGE, Facultad de Ciencias Exactas y Naturales, Universidad de Buenos Aires, Int. Guiraldes 2160, Buenos Aires, Argentina.
3. Instituto Argentino de Nivología, Glaciología y Ciencias Ambientales (IANIGLA, CCT-CONICET Mendoza). Avda. Ruiz Leal s/n, Parque Gral. San Martín, 5500 Mendoza, Argentina.
4. Department of Ecology and Evolutionary Biology, University of Toronto. 25 Harbord Street, Toronto, ON M5S 3G5, Canada; Section of Palaeobiology, Department of Natural History, Royal Ontario Museum. 100 Queen's Park Crescent, Toronto, ON M5S 2C6, Canada.

Recibido: 5 de junio 2020 - **Aceptado:** 4 de septiembre 2020 - **Publicado:** 17 de noviembre 2020

Para citar este artículo: Timothy J. Gaudin, Susan Tuckniss, Alberto Boscaini, François Pujos, and Gerardo De Iuliis (2020). Cranial osteology and taxonomy of *Pronothrotherium* (Xenarthra, Folivora, Nothrotheriidae) from the late Miocene–early Pliocene of Catamarca Province (Argentina). *Publicación Electrónica de la Asociación Paleontológica Argentina* 20 (2): 55–82.

Link a este artículo: http://dx.doi.org/10.5710/PEAPA.04.09.2020.320

Asociación Paleontológica Argentina
Maipú 645 1° piso, C1006ACG, Buenos Aires
República Argentina
Tel/Fax (54-11) 4326-7563
Web: www.apaleontologica.org.ar

ISSN 2469-0228

PeAPA | Publicación Electrónica
ASOCIACIÓN PALEONTOLÓGICA ARGENTINA
Año 2020 - 20(2): 55–82 ARTÍCULO

CRANIAL OSTEOLOGY AND TAXONOMY OF *PRONOTHROTHERIUM* (XENARTHRA, FOLIVORA, NOTHROTHERIIDAE) FROM THE LATE MIOCENE–EARLY PLIOCENE OF CATAMARCA PROVINCE (ARGENTINA)

TIMOTHY J. GAUDIN[1], SUSAN TUCKNISS[1], ALBERTO BOSCAINI[2], FRANÇOIS PUJOS[3], AND GERARDO DE IULIIS[4]

[1]Department of Biology, Geology and Environmental Science (Department 2653), University of Tennessee at Chattanooga. 615 McCallie Avenue, Chattanooga, TN 37403-2598, USA. *Timothy-Gaudin@utc.edu*

[2]División Paleontología Vertebrados, Museo de La Plata, Unidades de Investigación Anexo Museo. Facultad de Ciencias Naturales y Museo, Calle 60 y 122, 1900 La Plata, Argentina; and, Instituto de Ecología, Genética y Evolución de Buenos Aires (IEGEBA – CONICET). DEGE, Facultad de Ciencias Exactas y Naturales, Universidad de Buenos Aires, Int. Guiraldes 2160, Buenos Aires, Argentina. *alberto.boscaini@gmail.com*

[3]Instituto Argentino de Nivología, Glaciología y Ciencias Ambientales (IANIGLA, CCT-CONICET Mendoza). Avda. Ruiz Leal s/n, Parque Gral. San Martín, 5500 Mendoza, Argentina. *fpujos@mendoza-conicet.gov.ar*

[4]Department of Ecology and Evolutionary Biology, University of Toronto. 25 Harbord Street, Toronto, ON M5S 3G5, Canada; Section of Palaeobiology, Department of Natural History, Royal Ontario Museum. 100 Queen's Park Crescent, Toronto, ON M5S 2C6, Canada. *gerry.deiuliis@utoronto.ca*

TJG: https://orcid.org/0000-0003-0392-5001; **AB:** https://orcid.org/0000-0002-8666-9340; **FP:** https://orcid.org/0000-0002-6267-3927

Abstract. *Pronothrotherium typicum* is a late Miocene–early Pliocene (Huayquerian–Chapadmalalan SALMA) nothrotheriid sloth known from the Catamarca Province of northwestern Argentina. *Pronothrotherium* is one of four nothrotheriid genera known from relatively complete skeletal material, but unlike the other three, the osteology of *Pronothrotherium* has not been formally described. The present study provides the first detailed description and illustration of the cranial anatomy of *Pronothrotherium*, based largely on a nearly complete, subadult skull of *P. typicum* from the collections of The Field Museum (Chicago, Illinois, USA), as well as a less well-preserved adult skull and isolated mandible from the same collections. A revised cranial diagnosis of *P. typicum* is provided in the text. The skull of this species shows a number of distinctive features, most notably a peculiar vomerine keel in the nasopharynx, terminating in a swollen knob, that is, as far we know, a unique morphology among mammals. Based on the results of the present study, there appears to be reason to recognize two contemporaneous species of *Pronothrotherium*, *P. typicum* and *P. mirabilis*, although the latter is less well supported. We do not accept the validity of a third described species, *P. figueirasi,* considering it instead to be synonymous with *P. mirabilis.* The present study does not resolve the uncertain phylogenetic relationships among the well-preserved nothrotheriine taxa *Pronothrotherium*, *Mionothropus* (late Miocene), and the two Pleistocene genera in Nothrotheriini, *Nothrotherium* and *Nothrotheriops.* However, we hope that the data provided will facilitate subsequent phylogenetic studies that may resolve these issues.

Key words. Xenarthrans. Sloths. *Pronothrotherium.* Skull. Taxonomy.

Resumen. OSTEOLOGÍA CRANEANA Y TAXONOMÍA DE *PRONOTHROTHERIUM* (XENARTHRA, FOLIVORA, NOTHROTHERIIDAE) DEL MIOCENO TARDÍO–PLIOCENO TEMPRANO DE LA PROVINCIA DE CATAMARCA (ARGENTINA). *Pronothrotherium typicum* es un perezoso notrotérido del Mioceno tardío–Plioceno temprano (Edades Mamífero Huayqueriense–Chapadmalense) de la provincia de Catamarca, noroeste de Argentina. *Pronothrotherium* es uno de los cuatro géneros de notroterinos cuyos esqueletos son relativamente completos, pero a diferencia de los otros tres, su anatomía no ha sido formalmente descripta. El presente estudio proporciona las primeras descripciones e ilustraciones de la anatomía craneana de *Pronothrotherium*, basadas principalmente en un cráneo casi completo de un subadulto y un fragmento de cráneo de un adulto de *P. typicum*, depositados en las colecciones del Field Museum (Chicago, Illinois, USA). Se provee también una revisión de la diagnosis de *P. typicum* basada en caracteres craneanos. El cráneo de esta especie muestra una serie de características específicas, como una marcada quilla del vómer en la región nasofaríngea que termina en una protuberancia globosa, que representaría una característica única dentro de los mamíferos. Sobre la base del presente estudio se reconocen dos especies contemporáneas del género *Pronothrotherium*, *P. typicum* y *P. mirabilis*, aunque la segunda es más dudosa. No se acepta la validez de una tercera especie anteriormente descripta, *P. figueirasi*, que es considerada como sinónimo de *P. mirabilis.* Este estudio no se propone resolver las relaciones filogenéticas inciertas entre los notroterinos más conocidos *Pronothrotherium*, *Mionothropus* (Mioceno tardío) y los dos géneros de Nothrotheriini pleistocenos, *Nothrotherium* y *Nothrotheriops.* Sin embargo, esperamos que los datos proporcionados faciliten futuros estudios que abarquen estas cuestiones.

Palabras clave. Xenartros. Perezosos. *Pronothrotherium.* Cráneo. Taxonomía.

The extinct Nothrotheriidae is the smallest of the five widely recognized sloth clades (Gaudin, 2004; McDonald & De Iuliis, 2008; Pujos *et al.*, 2017; Boscaini *et al.*, 2019; Varela *et al.*, 2019; but see Delsuc *et al.*, 2019; Presslee *et al.*, 2019). The group incorporates perhaps seven undisputed genera (*i.e.*, *Pronothrotherium*, *Mionothropus*, *Lakukullus*, *Aymaratherium*, *Nothropus*, *Nothrotheriops*, and *Nothrotherium*), ranging in age from the middle Miocene (*Lakukullus*, Laventan SALMA –South American Land Mammal Age– Bolivia; Pujos *et al.*, 2014) to the Pleistocene (*Nothrotherium,* Brazil and Uruguay; and *Nothrotheriops*, North and central America, with a probable record in Argentina; McDonald & De Iuliis, 2008; Brandoni & Vezzosi, 2019). Craniodental remains of the Pleistocene taxa such as *Nothrotherium* and *Nothrotheriops* are fairly abundant. This is not the case, however, for the three undisputed nothrotheriids represented solely by isolated lower jaws (*Nothropus*, Burmeister, 1882; Ameghino, 1907; Brandoni & McDonald, 2015; *Lakukullus*, Pujos *et al.*, 2014; *Aymaratherium*, Pujos *et al.*, 2016). A wide variety of other sloth taxa have been linked phylogenetically to nothrotheriids, including the aquatic thalassocnine sloths lineage comprised of five species (Muizon & McDonald, 1995; McDonald & Muizon, 2002; Muizon *et al.*, 2003, 2004; De Iuliis *et al.*, 2011; Varela *et al.*, 2019), as well as an\assemblage of plesiomorphic late early Miocene sloths (*e.g.*, *Schismotherium*, *Hapalops*, *Analcimorphus*) from the Santacrucian SALMA. Phylogenetic analysis, however, has called these alliances into question. Amson *et al.* (2017) hypothesized that the thalassocnine sloths are more closely related to megatheriids than to nothrotheriids. Gaudin (2004) and Varela *et al.* (2019) showed that the Santacrucian sloths form a paraphyletic assemblage at the base of the clade Megatherioidea, the latter grouping including Megatheriidae, Nothrotheriidae, and Megalonychidae. Gaudin (2004) suggested provisionally referring to these Santacrucian taxa collectively as "basal megatherioids".

Although Nothrotheriidae is a small clade of sloths in terms of the number of taxa it incorporates, several of those taxa are very well known anatomically and are represented by several complete skeletons that have been described in great detail. This is especially true of the Pleistocene forms *Nothrotherium* and *Nothrotheriops* (Reinhardt, 1878; Stock 1925; Lull, 1929; Wilson, 1942; Cartelle & Fonseca, 1983; Cartelle & Bohórquez, 1986; Naples, 1990; Cartelle, 2012). Additionally, much of the anatomy of the late Miocene form *Mionothropus* is now known due to a detailed study of a single nearly complete specimen by De Iuliis *et al.* (2011). The subject of the present contribution, the late Miocene–early Pliocene *Pronothrotherium typicum* Ameghino, 1907 (Huayquerian–Chapadmalalan SALMA; McDonald & De Iuliis, 2008), is also represented by extensive remains. This species has been used frequently in phylogenetic analyses

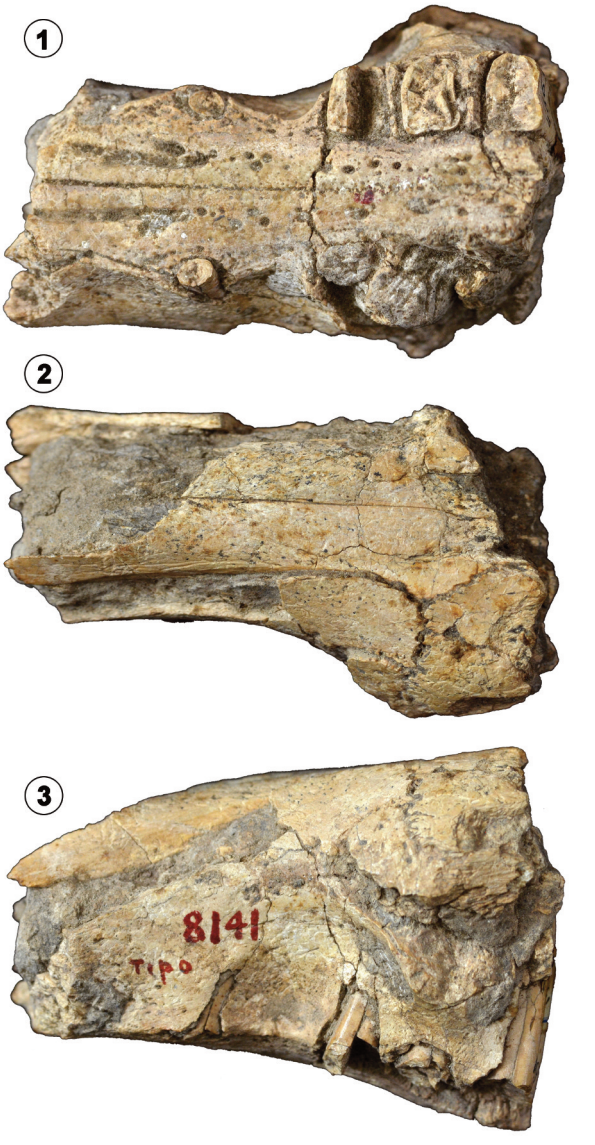

Figure 1. Photographs of the partial skull of ***Pronothrotherium typicum*, MACN-Pv 8141** (holotype). **1,** ventral view. **2,** dorsal view. **3,** left lateral view. Scale bar= 5 cm.

(Gaudin, 1995; Muizon & McDonald, 1995; McDonald & Muizon, 2002; Muizon *et al.*, 2003; Gaudin, 2004; De Iuliis *et al.*, 2011; Pujos *et al.*, 2016; Amson *et al.*, 2017; Varela *et al.*, 2019) where much of its anatomy has been coded into character matrices but, unfortunately, very little has ever been formally described.

The type specimen was described and illustrated successively by Ameghino (1907) and Rovereto (1914). The specimen includes the front end of the snout (Fig. 1) and the anterior portion of the mandible, including the upper and lower tooth rows and most of the mandibular spout. Riggs and Patterson (1939) recovered abundant materials of *Pronothrotherium* from the late Miocene–early Pliocene Andalhualá (= "Araucanense" of Riggs & Patterson, 1939) and Corral Quemado formations in the Villavil-Quillay Basin of Catamarca Province, Argentina (Fig. 2; Huayquerian–Montehermosan SALMA; Reguero & Candela, 2011; Bonini *et al.*, 2017). These fossils, housed in The Field Museum (Chicago, Illinois, USA), include skeletal remains of various individuals, among them several well preserved skulls and a nearly complete skeleton that has been on exhibit at the museum for many decades. This material has never been formally described, however, with the exception of a detailed report by Patterson *et al.* (1992) on the bony anatomy of the auditory region. Perea (1988) named a new species of *Pronothrotherium*, *P. figueirasi* Perea, 1988 (Huayquerian–Montehermosan SALMA, Uruguay) based on an isolated partial left mandible. He also assigned a poorly preserved skull and partial left mandible to *Pronothrotherium mirabilis*, a taxon previously represented by an isolated edentulous mandible from the late Miocene of Entre Ríos Province, Argentina (Kraglievich, 1925) originally assigned to the genus *Senetia*, which was subsequently synonymized with *Pronothrotherium* (Riggs & Patterson, 1939 –see also Brandoni, 2013). Perea (1988: lam. 1) supplied a photograph and brief description for each taxon, but ultimately provided

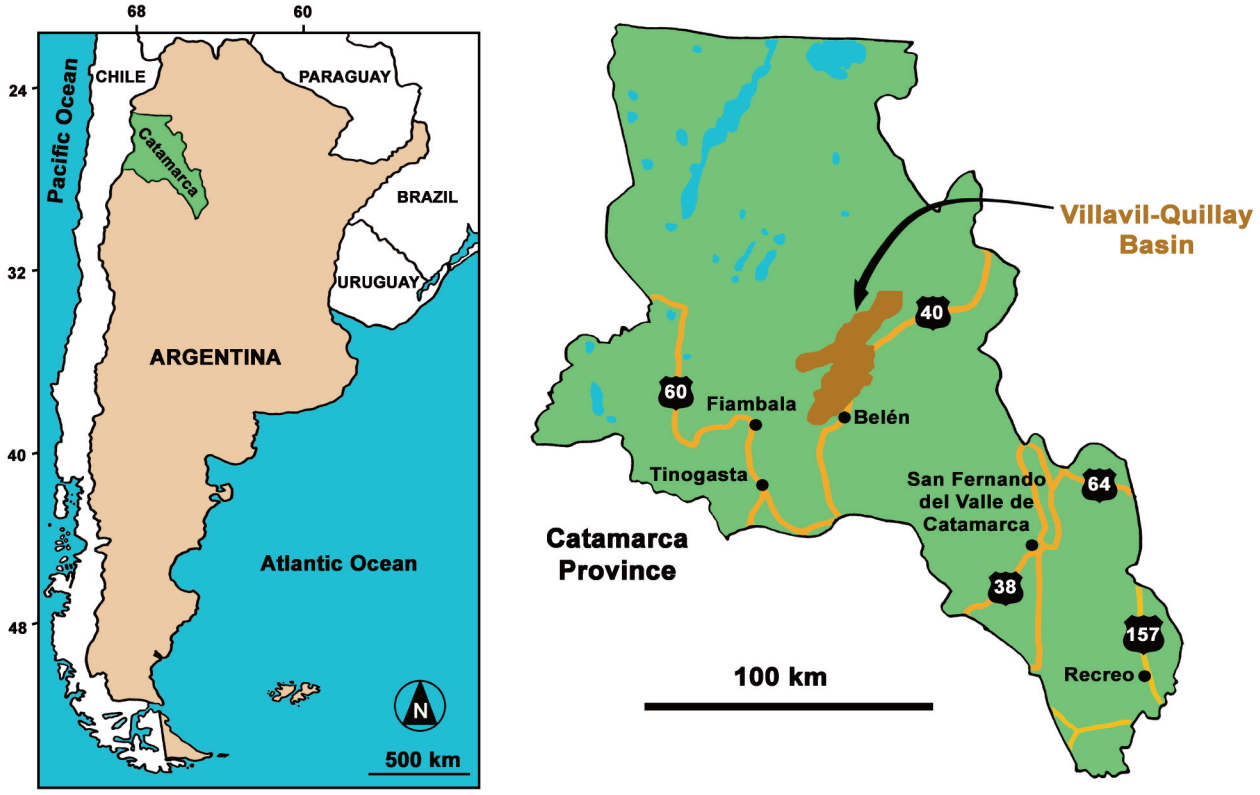

Figure 2. Left, general location map showing the Province of Catamarca in Argentina; right, close-up map of Catamarca Province, showing the location of the Villavil-Quillay Basin from which the fossils of *Pronothrotherium typicum* were recovered. Modified from Bonini *et al.* (2017).

little additional information on the anatomy of this genus.

It is certainly possible that the dearth of published information on *Pronothrotherium* anatomy has hindered resolution of its phylogenetic relationships. Although recent cladistic studies have strongly supported the monophyly of the Pleistocene nothrotheriids *Nothrotherium* and *Nothrotheriops* (Muizon & McDonald, 1995; McDonald & Muizon, 2002; Muizon *et al.*, 2003; Gaudin, 2004; De Iuliis *et al.*, 2011; Pujos *et al.*, 2016; Amson *et al.*, 2017; Varela *et al.*, 2019), the relationships of the other two well preserved nothrotheriids, *Pronothrotherium* and *Mionothropus*, to these two taxa have remained difficult to resolve. In some studies, one of the older representatives of the clade, the late Miocene *Mionothropus*, has been allied as the closest relative to the two Pleistocene taxa (Muizon & McDonald, 1995; Amson *et al.*, 2017; Varela *et al.*, 2019). By contrast, in perhaps the most detailed study of the matter and the one most focused on nothrotheriid relationships, De Iuliis *et al.* (2011) allocated the younger Mio–Pliocene *Pronothrotherium* to the position of sister taxon to the Pleistocene taxa. Still other studies have joined *Pronothrotherium* and *Mionothropus* to one another as sister taxa (McDonald & Muizon, 2002; Muizon *et al.*, 2003), or simply failed to unambiguously resolve their relationships (Perea, 1999; Gaudin, 2004; Pujos *et al.*, 2016).

For years, two of the authors of the present study (TJG and GDI) have collaborated on a long-term study of the extensive fossil remains of *Pronothrotherium* housed at The Field Museum, with the goal of publishing extensive descriptions and illustrations of all this material. Unfortunately, work on other projects has prevented us from completing this task. Although our study of the postcranial skeleton of *Pronothrotherium* is incomplete but ongoing, we decided that the description and detailed illustrations of cranial osteology and endocranial anatomy that we have completed were in themselves a valuable contribution. Therefore, the goal of the present contribution is to provide a detailed, well-illustrated description of the skull and mandible of *Pronothrotherium*, and to provide detailed comparisons of its anatomy to that of other nothrotheriids. It is our hope that this contribution will eventually lead to greater phylogenetic resolution within this important and poorly known group of extinct sloths.

MATERIALS AND METHODS

The descriptions below are based almost entirely upon a subadult specimen of *Pronothrotherium typicum*, FMNH P14467 (Figs. 3, 5–9). This is a well-preserved skull, lacking a mandible, with clearly visible sutures. Measurements for this skull are provided in Table 1. A second skull is part of the exhibit specimen FMNH P14503 (Fig. 4). It represents an adult skull with a mandible almost entirely reconstructed in plaster. Unfortunately, because of its status as an exhibit specimen, it was not available for detailed study, although we did have brief access to take several measurements and photographs. It is used to supplement the descriptions below, as needed. The description of the lower jaw below is based largely on an isolated mandibular specimen, FMNH P14350 (Fig. 10). All of The Field Museum material of *Pronothrotherium typicum* derives from the Andalhualá and Corral Quemado formations of Catamarca Province, northwestern Argentina (Fig. 2; Riggs & Patterson, 1939; Marshall & Patterson, 1981; Reguero & Candela, 2011; Esteban *et al.*, 2014; Bonini *et al.*, 2017; late Miocene–early Pliocene, Huayquerian–Montehermosan SALMA).

We collected X-ray micro-computed tomography (μCT) data for the skull of *Pronothrotherium typicum* FMNH 14467 at the University of Chicago PaleoCT Facility. The skull was scanned in a GE v|tome|x 240 scanner, using an acceleration voltage of 125 kV, an e-beam current of 200 μA and a 0.3 mm filter. A total of 1400 image slices were produced, resulting in isotropic voxel sizes of 117.137 μm. The tomographic data was later processed using the software Materialize Mimics v.21. Due to strong compactness of the sediment inside the skull, 3D digital models of the endocranial cavities were not reconstructed. However, the morphology of the main sinuses was directly observed on the tomographic images at representative coronal sections. A digital model of the external cranial morphology has been reconstructed and is available as a ".ply" file in Appendix 1 (Suppl. Information).

The skull of *Pronothrotherium typicum* is compared to the rather poorly preserved skull of *P. mirabilis* (FHC-DPV 271, Perea, 1988; late Miocene of Uruguay, Huayquerian SALMA), as well as to those of the other well-preserved, undoubted nothrotheriid species: *Mionothropus cartellei* (Frailey, 1986; De Iuliis *et al.*, 2011; late Miocene of Peru, Huayquerian

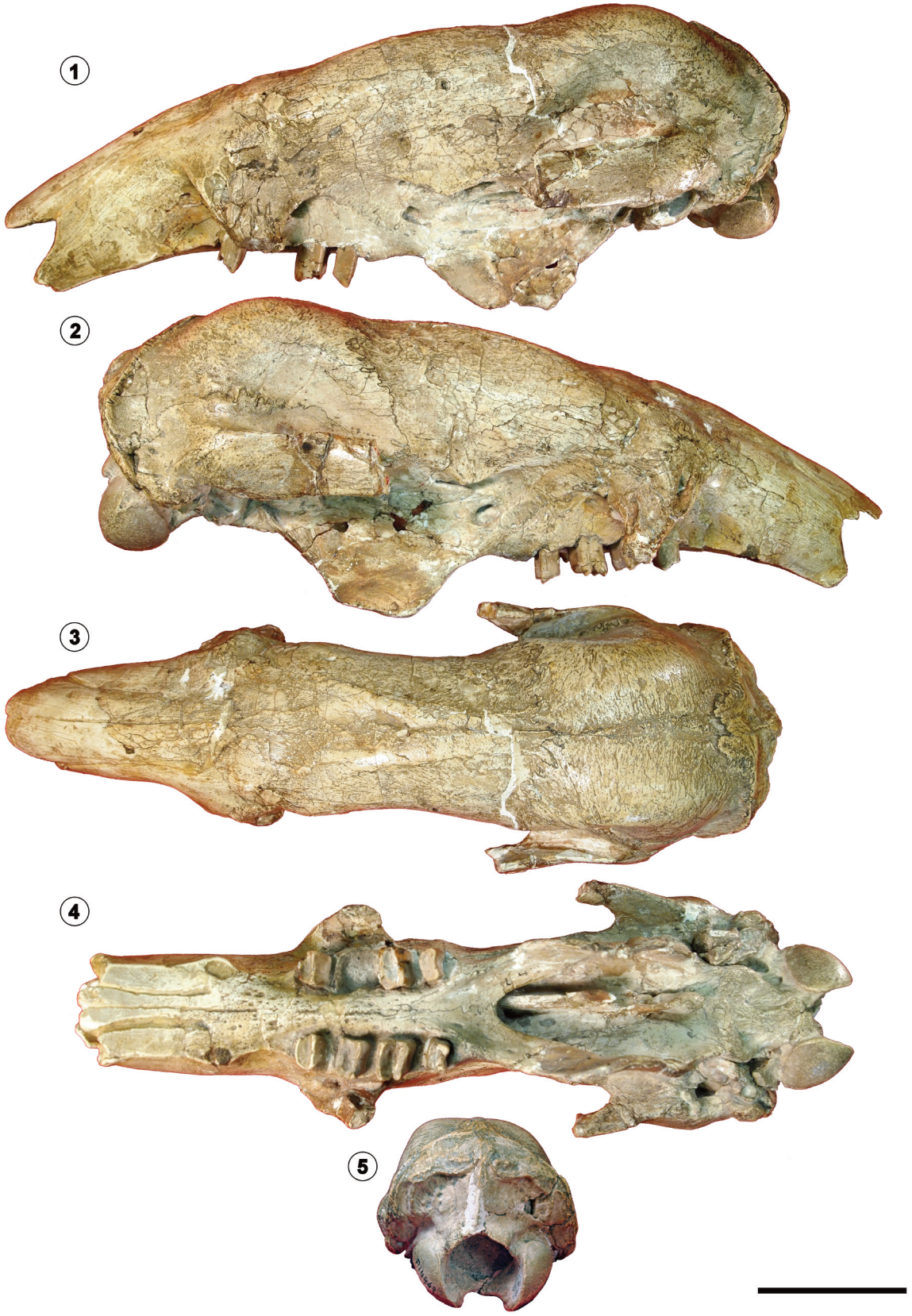

Figure 3. Photographs of the skull of ***Pronothrotherium typicum***, **FMNH P14467** (subadult). **1,** left lateral view. **2,** right lateral view. **3,** dorsal view. **4,** ventral view. **5,** posterior view. Scale bar= 5 cm.

TABLE 1 – Measurements of skull of *Pronothrotherium typicum* (FMNH P14467)*.

Skull measurements	
CML–length from post edge of occipital condyle to mes edge of Mf1	170.0
Length from postcondyle to mes edge of Cf1	195.0
Median-ventral length from ant edge of foramen magnum to ant edge of postpalatine notch	100.3
Median ventral length from ant edge of postpalatine notch to mes edge of Cf1	83.8
Diastema length (length between dist Cf1 and mes Mf1)	19.5
Molariform tooth row length (mes Mf1 to dist Mf4, L)	42.1
Min distance between dist edge of Mf4 and ant edge of postpalatine notch	18.9
Max width between labial edges of R and L Mf1	35.0
Max width between labial edges of R and L Mf	36.0
Ant Palatal width (min width in diastema between Cf1 and Mf1)	21.9
Mid-palatal width (min width between lingual edges of Mf1)	14.0
Post-palatal width (min width between lingual edges of Mf4)	17.1
Max width between lateral margins of infraorbital foramina	46.8
Max width between post edges of lacrimal foramina in dorsal view	61.7
Max width between frontal postorbital processes	52.1
Min interorbital width	45.3
Max width of occiput	69.4
Max width between lateral margins of occipital condyle	48.8
Max height of occipital condyle (L) in ventral view	25.6
Max width of foramen magnum	22.9
Median height of occiput (from dorsal edge of foramen magnum to dorsal margin of supraoccipital)	45.7
Length from postorbital process of frontal to dorsal nuchal crest	123.0
Tooth measurements	
Cf1 (max mesio-distal length)/Cf1 (max labio-lingual width)	6.8/4.6
Mf1 (max mesio-distal length)/Mf1 (max labio-lingual width)	7.4/10.3
Mf2 (max mesio-distal length)/Mf2 (max labio-lingual width)	8.1/11.4
Mf3 (max mesio-distal length)/Mf3 (max labio-lingual width)	9.1/11.7
Mf4 (max mesio-distal length)/Mf4 (max labio-lingual width)	6.1/8.7

*All measurements in millimeters. Palatal measurements do not include the missing premaxilla. Abbreviations: **CML,** condylar–molariform length; **ant,** anterior; **Cf1,** upper caninform tooth; **dist,** distal; **L,** left side of skull; **max,** maximum; **mes,** mesial; **Mf,** upper molariform tooth; **min,** minimum; **post,** posterior; **R,** right side of skull.

SALMA), *Nothrotherium maquinense* (Reinhardt, 1878; Kraglievich, 1926; Paula Couto, 1971; Cartelle & Fonseca, 1983; Cartelle & Bohórquez, 1986; Perea, 2007; Cartelle, 2012; Pleistocene of Argentina, Brazil, and Uruguay, Lujanian SALMA), and *Nothrotheriops shastensis* (Stock, 1925; Lull, 1929; Wilson, 1942; Naples, 1990; De Iuliis *et al.*, 2015; Pleistocene of southwest USA, Mexico and northern Central America, Irvingtonian and Rancholabrean NALMA–North

American Land Mammal Age). The basal megatherioid genus *Hapalops* (Scott, 1903, 1904; late early Miocene throughout much of South America, Santacrucian SALMA) is also used in the comparisons to provide polarity information.

In the description of the *P. typicum* mandible, additional nothrotheriids known only from mandibular specimens are included in the comparisons: the type of *P. figueirasi* (FHC-DPV 270, Perea, 1988: lam. 1; early Pliocene of Uruguay, Montehermosan SALMA); the type of *P. mirabilis* (MACN-Pv 1013, late Miocene of Argentina, Montehermosan SALMA); the three described species of the genus *Nothropus* (*N. carcaranensis*, *N. priscus*, and *N. tarijensis*; Burmeister, 1882; Ameghino, 1907; Brandoni & McDonald, 2015; Pleistocene of Argentina and Bolivia, Lujanian SALMA); *Lakukullus anatirostratus* (Pujos *et al.*, 2014; middle Miocene of Bolivia, Laventan SALMA); and *Aymaratherium jeani* (Pujos *et al.*, 2016; early Pliocene of Bolivia, Montehermosan SALMA).

A description of the bones of the auditory region is not included in the present study. This region of the skull of FMNH P14467, including the ectotympanic, entotympanic, and petrosal bones, has already been described and illustrated in detail by Patterson *et al.* (1992). There are no preserved ear ossicles among the FMNH material of *Pronothrotherium*.

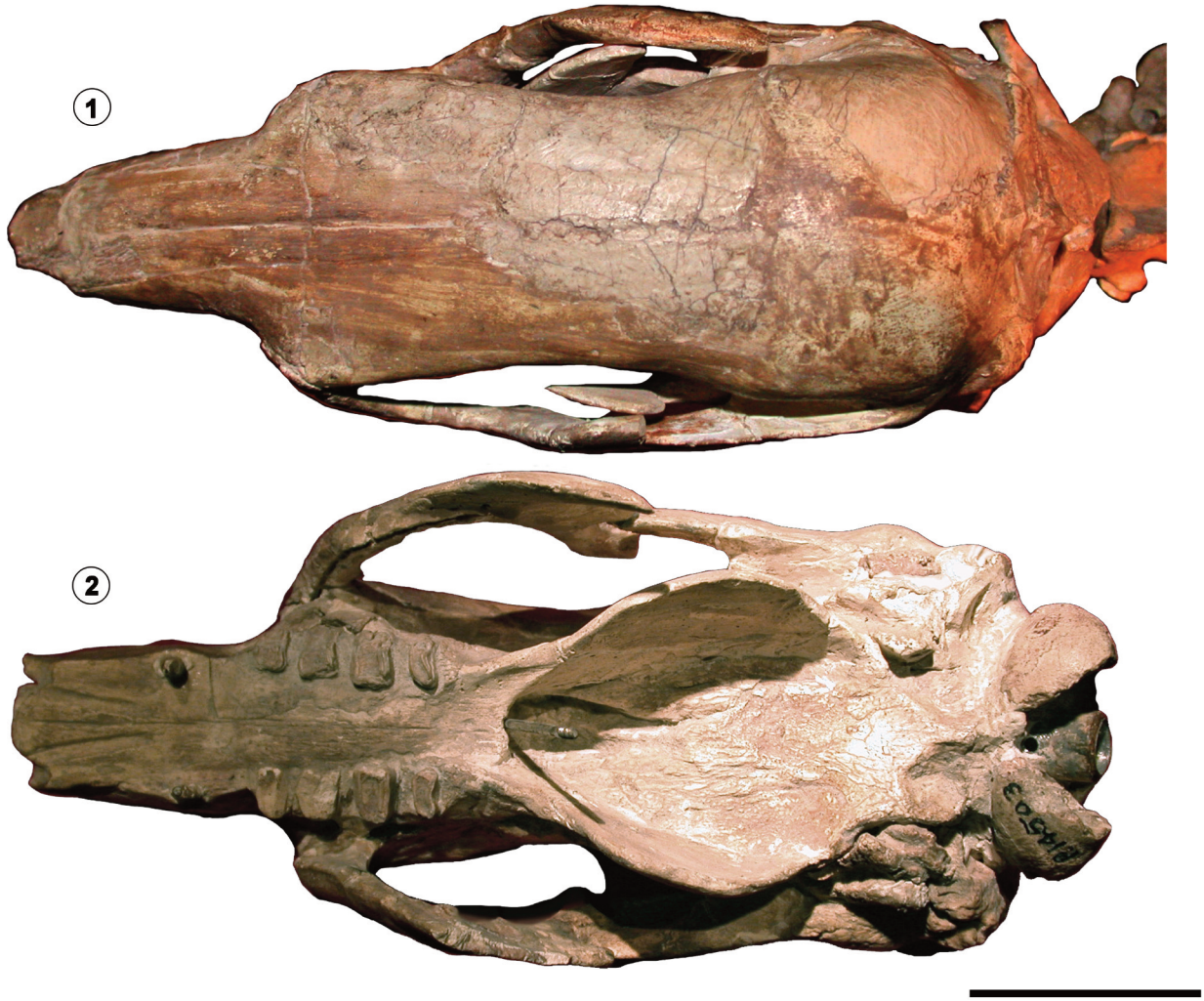

Figure 4. Photographs of the skull of ***Pronothrotherium typicum***, **FMNH P14503**. **1,** dorsal view. **2,** ventral **v**iew. Scale bar= 5 cm.

The anatomical terminology utilized in the present study follows that of Wible and Gaudin (2004), De Iuliis *et al.* (2011), and Gaudin (2011). Measurements for all specimens were taken with a digital caliper to the nearest 0.1 mm.

Acronyms. AMNH, American Museum of Natural History, New York, USA; **FMNH,** The Field Museum, Chicago, USA; **FHC-DPV,** Colección del Departamento de Paleontología, Facultad de Humanidades y Ciencias, Universidad de la República, Montevideo, Uruguay; **LACMHC,** Hancock Collection, George C. Page La Brea Tar Pit Museum, Los Angeles County Museum of Natural History, Los Angeles, USA; **MACN-Pv,** Museo Argentino de Ciencias Naturales "Bernardino Rivadavia", Colección Nacional de Paleovertebrados, Buenos Aires, Argentina.

Other abbreviations. Cf/cf, upper/lower caniniform tooth; **CML,** condylar-molariform length; **ln.,** anteroposterior length; **Mf/mf,** upper/lower molariform tooth; **wd.,** transverse width.

SYSTEMATIC PALEONTOLOGY

XENARTHRA Cope, 1889
FOLIVORA Delsuc, Catzefelis, Stanhope & Douzery, 2001
NOTHROTHERIIDAE Gaudin, 1994
NOTHROTHERIINAE Ameghino, 1920

Genus ***Pronothrotherium*** Ameghino, 1907

Type species. *Pronothrotherium typicum* Ameghino, 1907. Late Miocene–early Pliocene, Argentina.

Pronothrotherium typicum Ameghino, 1907
Figures 1, 3–10

Revised cranial diagnosis. Small nothrotheriine sloth with unique, unambiguous cranial synapomorphies of Nothrotheriinae noted in De Iuliis *et al.* (2011), including posteriorly expansive vomerine exposure in nasopharynx; deep, elongated, asymmetrical ventral vomerine keel extending posteriorly into the nasopharynx; posterior root of zygoma directed anteriorly; hypertrophied ventral nuchal crest; and short and broad coronoid process (ratio of maximum height to anteroposterior length measured at mid-height <1.0); but, lacking apomorphies of Nothrotheriini noted by De Iuliis *et al.* (2011), including single pair of enlarged postpalatal foramina and presence of osseous pterygoid bulla. Cranial autapomorphies include deep groove on distal surface of Mf4, low sagittal crest, descending lamina of pterygoid with squared corners in lateral view, a distinctive vomerine ridge, with a ventral edge folded to the left so that the ridge is convex on the left and concave on the right, terminating in an swollen, bulb-like process. Distinguished from *P. mirabilis* by larger size and elongated postpalatal shelf.

Type material. MACN-Pv 8141, anterior skull and partial mandible.

Referred material. FMNH P14503, partial skull, mandible and skeleton; (exhibit specimen); FMNH P14467, subadult skull with associated postcranial remains; FMNH P14350, mandible, including nearly complete left and right dentaries.

DESCRIPTION

Skull

Premaxilla/maxilla. No trace of the premaxilla has been recovered in any of the specimens attributed to *Pronothrotherium*. However, most of the maxilla is known. In FMNH P14467, the posterior and ventral portions of the maxilla are well preserved on both sides (Figs. 5–7). Much of the anterior and dorsal maxilla is lost (although this region has been reconstructed in plaster by the original preparators, based on the type specimen; this region is missing as well from FMNH P14503, see Fig. 4). The right facial portion of the maxilla is preserved anteriorly to a point just in front of the caniniform (Cf1) alveolus, extending posteriorly and dorsally to include the entire lacrimal and jugal contact. The maxilla almost certainly contacted the frontal posterodorsally, but there is a small, plaster-filled crack lying in the area where this suture most likely was situated. A narrow section of the maxillonasal suture is preserved on the right from the level of the first molariform (Mf1) to Cf1. On the left side, only a small ventral region of the maxillary facial process is preserved, beginning just posterior to the caniniform alveolus and extending posteriorly to the jugal contact.

Both left and right facial portions of the maxilla contain a large buccinator fossa (Fig. 6). The fossa extends from the caniniform alveolus anteriorly to the first molariform

posteriorly. It is bounded ventrally by the lateral edge of the palate and rises dorsally to the level of the lacrimojugal contact. A well-developed buccinator fossa is present in *Hapalops* (Scott, 1903, 1904) and in *Mionothropus* (Frailey, 1986; De Iuliis *et al.*, 2011) but is lacking in *Nothrotheriops* (Stock, 1925) and *Nothrotherium* (Reinhardt, 1878; Cartelle & Fonseca, 1983; Cartelle, 2012).

The anterior region of the maxilla is missing from the palate beginning just anterior to Cf1 on the right side and just posterior to Cf1 on the left (Figs. 3.4, 5–6). The preserved portion of the right palatal process bears a large foramen opposite Cf1, the anterior palatal foramen, opening

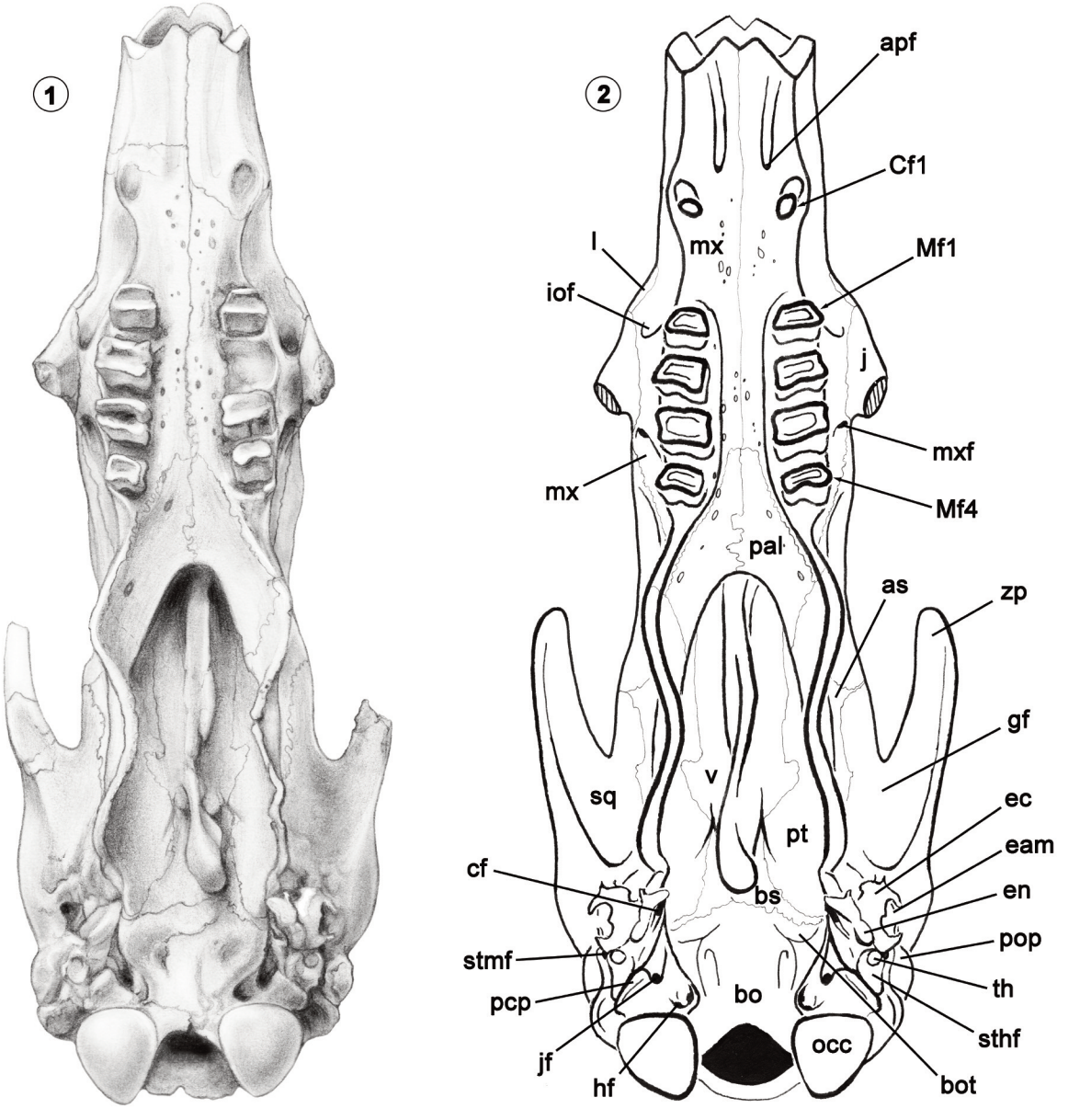

Figure 5. Skull of ***Pronothrotherium typicum***, **FMNH P14467**. **1,** grayscale drawing. **2,** labeled reconstruction. Abbreviations: **apf,** anterior palatal foramen; **as,** alisphenoid; **bo,** basioccipital; **bot,** basioccipital tuber; **bs,** basisphenoid; **Cf1,** upper caniniform; **cf,** carotid foramen; **eam,** external auditory meatus; **ec,** ectotympanic; **en,** entotympanic; **gf,** glenoid fossa; **hf,** hypoglossal foramen; **iof,** infraorbital foramen; **j,** jugal; **jf,** jugular foramen; **l,** lacrimal; **Mf1/4,** upper first/fourth molariform; **mx,** maxilla; **mxf,** maxillary foramen; **occ,** occipital condyle; **pal,** palatine; **pcp,** paracondylar process; **pop,** paroccipital process of petrosal (= mastoid process of Patterson *et al.* 1992); **pt,** pterygoid; **sq,** squamosal; **sthf,** stylohyal fossa; **stmf,** stylomastoid formen; **th,** tympanohyal; **v,** vomer; **zp,** zygomatic process of squamosal. Scale bar= 5 cm.

into a distinct groove, the anterior palatal groove, that extends to the preserved anterior edge of the maxilla (Fig. 5). The anterior palatal grooves and foramina are more completely preserved in the type specimen of *Pronothrotherium*

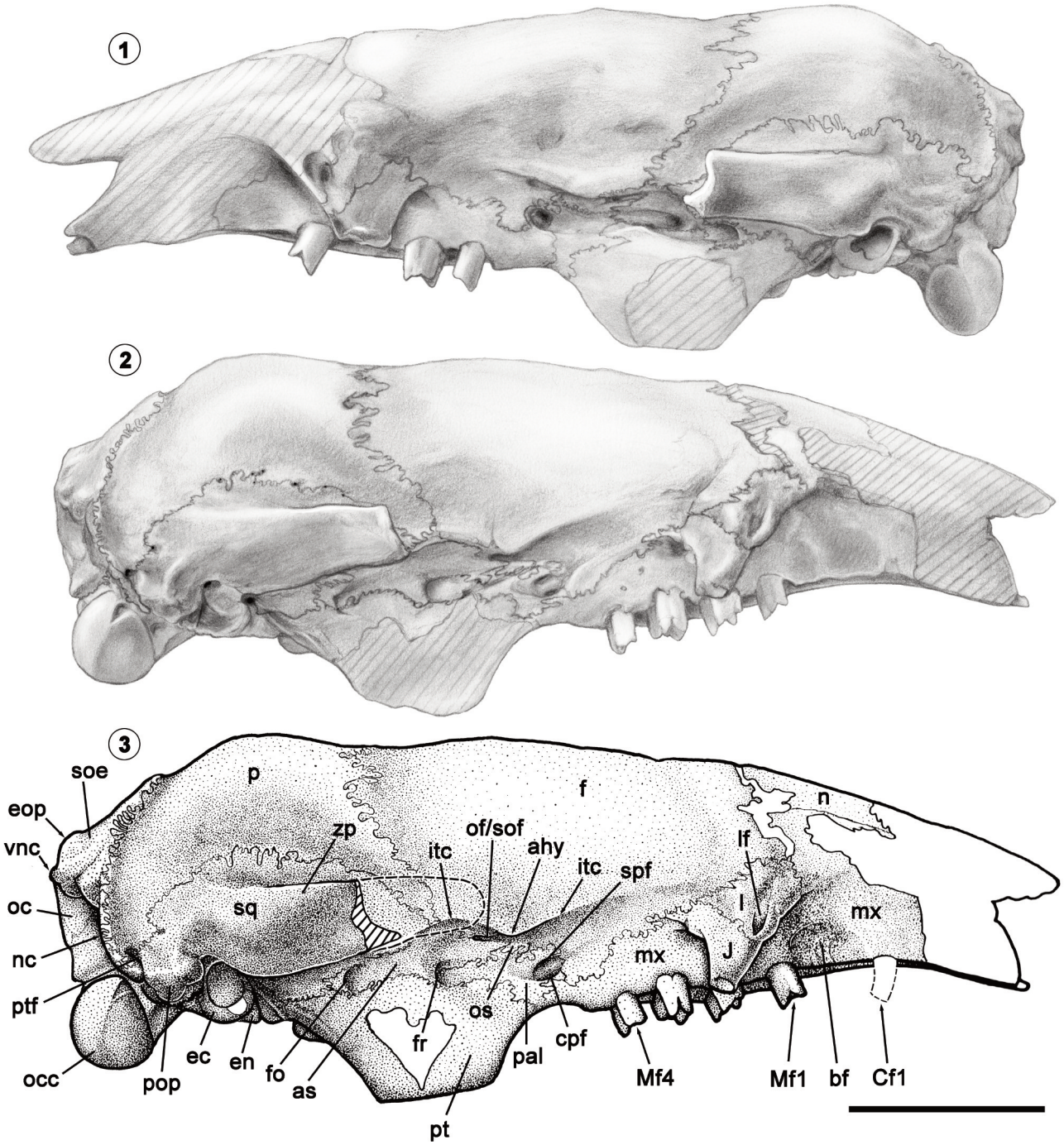

Figure 6. Skull of ***Pronothrotherium typicum***, **FMNH P14467**. **1,** left lateral view, grayscale drawing. **2,** right lateral view, grayscale drawing. **3,** right lateral view, labeled drawing. Abbreviations: **ahy,** ala hypochiasmata; **as,** alisphenoid; **bf,** buccinator fossa; **Cf1,** upper caniniform; **cpf,** caudal palatine foramen; **ec,** ectotympanic; **en,** entotympanic; **eop,** exoccipital protuberance; **f,** frontal; **fo,** foramen ovale; **fr,** foramen rotundum; **itc,** infratemporal crest; **j,** jugal; **l,** lacrimal; **lf,** lacrimal foramen; **Mf1/4,** upper first/fourth molariform; **mx,** maxilla; **n,** nasal; **nc,** nuchal crest; **oc,** occipital; **occ,** occipital condyle; **of/sof,** common aperture of optic foramen/sphenorbital fissure; **os,** orbitosphenoid; **p,** parietal; **pal,** palatine; **pop,** paroccipital process of petrosal (= mastoid process of Patterson *et al.* 1992); **pt,** pterygoid; **ptf,** posttemporal foramen; **soe,** dorsal supraoccipital exposure; **spf,** sphenopalatine foramen; **sq,** squamosal; **vnc,** ventral nuchal crest; **zp,** zygomatic process of squamosal. Scale bar= 5 cm.

typicum (Fig. 1; MACN-Pv 8141) illustrated by Ameghino (1907) and Rovereto (1914), showing that the grooves are well defined and quite elongated, as they are in other nothrotheriids (Stock, 1925; De Iuliis *et al.*, 2011). The anterior palatal foramina and grooves serve as anterior openings for the palatine canal, which travels through the palatine and maxilla, and contains the major palatine arteries, nerves, and blood vessels (Evans & Christensen, 1979). They are widely distributed in extinct and extant sloths, as well as some anteaters (Gaudin, 2004). As in other sloths (Gaudin, 2004), the surface of the palatal process is extensively pitted (Fig. 5). These pits represent foramina for minor branches of the major palatine vessels and nerves. The surface of the palatal process is relatively flat between

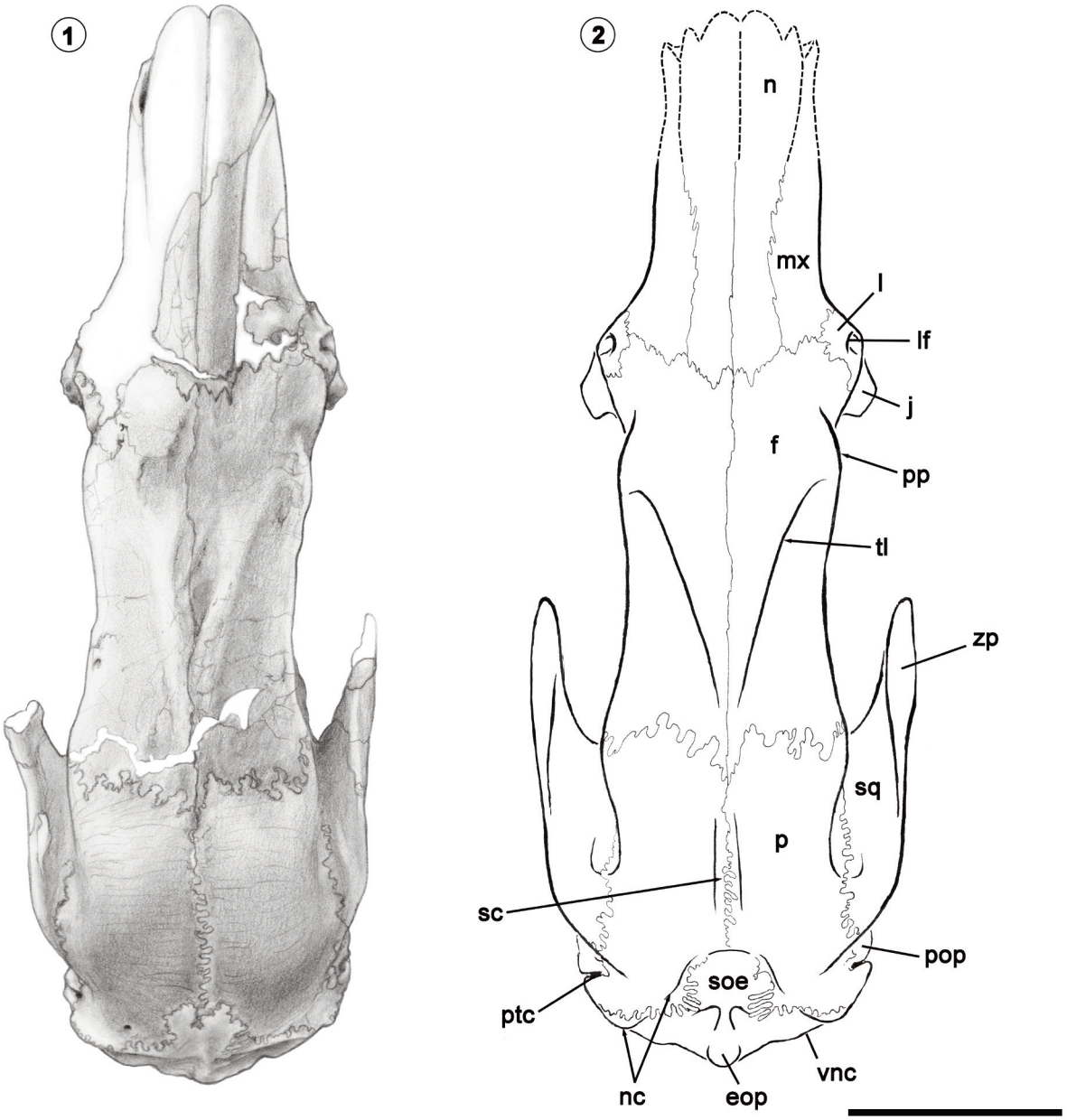

Figure 7. Skull of ***Pronothrotherium typicum***, **FMNH P14467**, in dorsal view. **1,** grayscale drawing. **2,** labeled reconstruction. Abbreviations: **eop,** exoccipital protuberance; **f,** frontal; **j,** jugal; **l,** lacrimal; **lf,** lacrimal foramen; **mx,** maxilla; **n,** nasal; **nc,** nuchal crest; **p,** parietal; **pop,** paroccipital process of petrosal (= mastoid process of Patterson *et al.* 1992); **pp,** postorbital process of frontal; **ptc,** posttemporal canal; **sc,** sagittal crest; **soe,** dorsal supraoccipital exposure; **sq,** squamosal; **tl,** temporal lines; **vnc,** ventral nuchal crest; **zp,** zygomatic process of squamosal. Scale bar= 5 cm.

the caniniform alveoli but becomes increasingly convex transversely as it extends posteriorly through the molariform region. From the small portion of the palatal process preserved anterior to the right Cf1, it is apparent that the snout of FMNH P14467 narrowed somewhat anterior to the caniniform, as in the type specimen (Fig. 1; MACN-Pv 8141; Rovereto, 1914). Posterior to Cf1, the lateral margin of the palatal process is strongly indented by the ventral margins of the buccinator fossa. The process then widens to accommodate the molariform teeth. Between the molariform tooth rows, the palate is narrow (wd.= 14.5 mm at the level of Mf3, 8.4% of CML). The palate of *Pronothrotherium typicum* is narrower than that of *Nothrotheriops shastensis* (wd.= 24.5 mm, 9.8% of CML —based on the cast of LACMHC 1800-3) and *Mionothropus cartellei* (10.5% of CML at narrowest point between molariforms —De Iuliis *et al.*, 2011), but similar in width to that of *Hapalops elongatus*, (wd.= 27.1 mm, 8.3% of CML —based on FMNH P13141). The maxillopalatine contact is V-shaped with the apex pointing anteriorly, as in *Nothrotheriops* (Stock, 1925) and *Nothrotherium* (Guth, 1961), but in contrast to *Mionothropus*, where the suture is squared off transversely (De Iuliis *et al.*, 2011).

The facial portion of the maxilla bears an infraorbital foramen just medial to the maxillojugal contact opposite the mesial edge of Mf2. The maxillary foramen lies within the base of the zygomatic process of the maxilla at the level of Mf3 (Fig. 5). The infraorbital canal of *Pronothrotherium* (ln.= 22 mm, 13% of CML) is similar in length to that of *Nothrotheriops* (ln.= 35 mm, 13.8% of CML —based on the cast of LACMHC 1800-3). The large orbital exposure of the maxilla is bounded by the jugal anterodorsally, the frontal posterodorsally, and the palatine posteriorly (Fig. 6). It is indented by a small, round depression immediately posterior to the alveolus of Mf4, a synapomorphy of megatherioid sloths (Gaudin, 2004). The maxilla also bears a distinct boss on the palatal margin just posterior to Mf4.

Upper dentition. *Pronothrotherium* differs from *Nothrotheriops* (Stock, 1925) and *Nothrotherium* (Reinhardt, 1878; Cartelle & Fonseca, 1983) in its retention of a small caniniform separated by a wide diastema from the four molariform teeth (Figs. 5–6). In this respect it resembles *Mionothropus* (Frailey, 1986; De Iuliis *et al.*, 2011) and *Hapalops* (Scott, 1903, 1904). The alveolus of the right Cf1 has been preserved in FMNH P14467, but the left Cf1 is missing in its entirety (Fig. 5). The left Mf1, Mf4, and the right Mf3 are well preserved. The occlusal surfaces of the right Mf2, Mf4, and the left Mf3 are partially damaged. The left Mf2 is entirely absent. The right Mf1 is reconstructed in plaster, but it is unclear how much (if any) of the tooth itself is preserved (Figs. 3.4, 5). In FMNH P14503 (Fig. 4.2), only the left and right Mf3 and Mf4 are well-preserved. The left Mf1 and Mf2 and right Cf1 are partially preserved, missing much of their crowns, and the remaining teeth are entirely reconstructed in plaster. Rovereto (1914) suggested that the incomplete Cf1 preserved in the type was recurved posteriorly. The alveolar portion of the caniniform in both Field Museum specimens is cylindrical and compressed mediolaterally (Figs. 3.4, 5).

Mf1 is smaller than Mf2 and Mf3, which are similar in size. Mf4 is the smallest molariform (Fig. 5). As in other megatherioids (Gaudin, 2004), the molariforms bear mesial and distal transverse crests on their occlusal surfaces formed of wear-resistant orthodentine (Owen, 1856; Ferigolo, 1985; Bargo *et al.*, 2009; Kalthoff, 2011). Between these crests is a valley composed of softer, modified orthodentine (as well as a soft layer of cementum anterior and posterior to the two transverse crests; Owen, 1856; Ferigolo, 1985; Kalthoff, 2011). This orthodentine basin is worn deepest in the center. There is a low crest that connects the mesial and distal occlusal crests on the labial and lingual margins of each basin. The molariforms are compressed anteroposteriorly, and in general shape resemble those of other nothrotheriids (Reinhardt, 1878; Stock, 1925; Cartelle & Fonseca, 1983; Frailey, 1986; De Iuliis *et al.*, 2011). Mf1 is trapezoidal. In occlusal view the distal surface of the crown is planar and the mesial surface slightly convex. The distal occlusal crest is higher and wider transversely than the mesial crest. Unlike other nothrotheriids (Reinhardt, 1878; Stock, 1925; Cartelle & Fonseca, 1983; Frailey, 1986; De Iuliis *et al.*, 2011), the transverse width of the tooth is much greater than its mesiodistal length, and unlike *Mionothropus* (Frailey, 1986; De Iuliis *et al.*, 2011), its lingual and labial edges are subequal in length. Mf2 and Mf3 are similar in size and shape. They are quadrate with slightly rounded corners. In occlusal view their mesial sides are slightly convex and their distal sides are slightly concave.

The mesial crest of Mf3 is higher than the distal crest. The mesial crest is higher at its lingual end, whereas the distal crest is higher labially. As the occlusal surface of Mf2 is damaged, it is not possible to determine with certainty the relative height of the mesial and distal crests. In both Mf2 and Mf3, the lingual edge of the tooth is more elongated mesiodistally than the labial edge, as in other nothrotheriids (Reinhardt, 1878; Stock, 1925; Cartelle & Fonseca, 1983; Frailey, 1986; De Iuliis *et al.*, 2011). Mf4 is a small quadrate tooth with rounded corners that lacks a mesial transverse crest. Unlike Mf2 and Mf3, the distal surface of Mf4 bears a strong groove, forming a marked concavity on the distal occlusal margin. This groove is present but shallower in other nothrotheriids (Reinhardt, 1878; Stock, 1925; Cartelle & Fonseca, 1983; Frailey, 1986; De Iuliis *et al.*, 2011). The mesial side of Mf4 is slightly convex. Mf4 appears to be somewhat variable in outline among nothrotheriids. It is highly compressed mesiodistally in FMNH P14503 (Fig. 4.2), *Mionothropus* and some *Nothrotherium* specimens (Reinhardt, 1878), where it appears nearly triangular with a lingual apex, whereas it is deeper mesiodistally in FMNH P14467 (Fig. 5) and other *Nothrotherium* specimens (Cartelle & Fonseca, 1983; Cartelle & Bohórquez, 1986), and deeper still in *Nothrotheriops*, where it takes on a trapezoidal shape, with a mesial crest that is narrower transversely than the distal crest (Stock, 1925). A distinct apicobasal sulcus is present on the labial face of Mf2 and Mf3, and is present to a lesser extent on the lingual face. Mf4 shows a faintly developed apicobasal sulcus on both labial and lingual faces. The sulci appear to be absent on Mf1. These distinct apicobasal sulci are sometimes present labially in *Hapalops* (Scott, 1903, 1904; contra McDonald & Muizon, 2002) and are well developed lingually and labially in *Nothrotheriops* (Stock, 1925) and other nothrotheriids (as well as *Thalassocnus*; McDonald & Muizon, 2002). In lateral view, the molariform teeth of FMNH P14467 are directed anteriorly and ventrally (Figs. 3.1–3.2, 6). Mf4 is slightly recurved anteriorly, as in other nothrotheriids (Stock, 1925; De Iuliis *et al.*, 2011; Cartelle, 2012) and *Hapalops* (Scott, 1903, 1904).

Palatine. The palatal portion of the palatine lies posteromedial to the maxilla, extending anteriorly to a level opposite the distal edge of Mf3 (Fig. 5). The maxillopalatine suture of *Nothrotheriops* is also situated opposite Mf3 (LACMHC 1800-4), whereas in *Mionothropus* it extends farther forward to Mf2 (De Iuliis *et al.*, 2011). The palatine widens posteriorly and extends behind the distal edge of Mf4 to form a long postpalatal shelf. Indeed, the latter is much longer (ln.= 16 mm —from posterior edge of Mf4 to anterior edge of post-palatine notch—or 9.3% of CML in FMNH P14467) than that of *Nothrotheriops* (ln.= 15.5 mm, 6.7% of CML —based on LACMHC 1800-11). It also appears to be longer than that of *Pronothrotherium mirabilis* (Perea, 1988) or *Nothrotherium* (Reinhardt, 1878; Cartelle & Fonseca, 1983), whereas in *Mionothropus* (De Iuliis *et al.*, 2011) and *Hapalops* (Scott, 1903, 1904) the shelf is absent. The shelf terminates medially at the U-shaped post-palatine notch but continues laterally along the medial edge of the descending pterygoid laminae for nearly 1/3 of their anteroposterior length. The lateral portion of the postpalatal shelf contacts the pterygoid posteriorly. The postpalatal shelf bears a series of small post-palatal foramina; three on the right side and two on the left (Figs. 3.4, 5). In this respect, FMNH P14467 differs from *Pronothrotherium mirabilis* (Perea, 1988), in which the postpalatal shelf bears a pair of single large foramina. *Nothrotheriops* also has a single pair of large foramina, as well as several smaller post-palatal foramina (Stock, 1925; Lull, 1929).

The medial surface of the palatine's perpendicular lamina forms the lateral wall of the nasopharynx. It is not well exposed, being largely covered by matrix, but it appears to be excluded from the roof of the nasopharynx by the vomer. The lateral surface of this perpendicular lamina participates in the medial wall of the orbit. This orbital exposure begins ventrally as a narrow bridge connecting to the palatal shelf and expands dorsally into the orbit roughly in the form of an inverted triangle (Fig. 6.2–6.3), much like that of *Mionothropus* (De Iuliis *et al.*, 2011) and *Nothrotheriops* (LACMHC 1800-6). It contacts the alisphenoid, orbitosphenoid, and frontal dorsally and extends nearly to the ventral edge of the sphenorbital fissure/optic foramen. It contacts the pterygoid posteroventrally and the maxilla anteroventrally. It bears the sphenopalatine fossa in its anterodorsal corner along its contact with the frontal. Two foramina are present in this fossa. We identify these as a more dorsal sphenopalatine foramen and a more ventral caudal palatine foramen, as in *Mionothropus* (De Iuliis *et al.*, 2011) and the

Antillean megalonychid sloth *Neocnus* (Gaudin, 2011). The two are separated by a narrow bridge of bone within the fossa. The position of the posterior suture between the palatine and the alisphenoid is difficult to determine. The palatine may have a small participation in the anteroventral rim of the foramen rotundum depending upon the location of this contact.

Nasal. Only the posterior half of the nasals are preserved in FMNH P14467 (Figs. 3.3, 6–7). The anterior portions are reconstructed in plaster. The anterior portion of the nasals are missing from the type as well (Fig. 1; MACN-Pv 8141), and the nasals are entirely absent in FMNH P14503 (Fig. 4.1). The right nasal is preserved from the frontonasal suture to the level of the mesial edge of the caniniform tooth. The left nasal is preserved anteriorly to the level of the distal edge of the caniniform tooth, but is extensively damaged laterally. A wide plaster-filled crack crosses both nasals transversely just anterior to the frontonasal suture. Only the right nasal preserves a portion of the lateral contact with the maxilla. It would appear from the preserved portion that this contact is concave laterally. The nasal is widest at the level of the frontomaxillary suture. It then narrows anteriorly before expanding laterally again anteriorly. The strongly laterally concave nasomaxillary contact in *Pronothrotherium* (Fig. 7) differs from the condition in *Nothrotheriops* (Stock, 1925: fig. 5) and *Nothrotherium* (Cartelle, 2012), where the nasals are of more uniform width and only slightly concave laterally, but resembles the condition in *Mionothropus* (De Iuliis *et al.*, 2011) and *Hapalops* (Scott, 1904: pl. 38). The nasals contact the frontals posteriorly and form a W-shaped suture with the middle apex pointing anteriorly (Fig. 7). The posteriormost point of the frontonasal suture lies at the level of Mf3.

Lacrimal. The lacrimal is almost completely preserved on the right side (Fig. 6.2–6.3). It has a small orbital and somewhat larger facial exposure. The anterodorsal corner of the facial exposure is slightly eroded. Only the orbital exposure is preserved on the left. The lacrimal is roughly triangular in lateral view. It contacts the maxilla anteriorly, the frontal dorsally, and the jugal ventrally. It is slightly larger than the small, quadrangular lacrimal of *Mionothropus* (De Iuliis *et al.*, 2011), but is much smaller than the lacrimal in *Nothrotherium* (Reinhardt, 1878) and *Nothrotheriops* (Stock, 1925), which have a larger orbital process that extends farther dorsally than that of *Pronothrotherium*. The lacrimal is perforated by a large lacrimal foramen near its anterior edge. In *Pronothrotherium* the anterior wall of the lacrimal foramen is elevated to form a sharp ridge (Fig. 6). This elevated anterior wall is similar to that seen in other nothrotheriids (Reinhardt, 1878; Stock, 1925; De Iuliis *et al.*, 2011) and in *Hapalops* (Scott, 1903, 1904). The posterior wall of the lacrimal foramen is rounded but does not form the distinct tubercle present in *Nothrotheriops* (Stock, 1925). The ventral edge of the lacrimal foramen develops into a groove extending ventrally and opening onto the surface of the lacrimal.

Jugal. The large orbital exposure of the jugal is preserved on both the left and right sides (Fig. 6). It is interposed between the lacrimal dorsolaterally and the maxilla ventromedially, excluding any orbital contact between the lacrimal and the maxilla, as in *Nothrotheriops* (Stock, 1925), as well as basal megatherioids, *Eucholoeops* and other megalonychids, *Bradypus*, and scelidotheriine mylodontids (Gaudin, 2004; Gaudin *et al.*, 2015; but see Boscaini *et al.*, 2020a). The jugal contacts the frontal posterodorsally. The base of the zygomatic process of the jugal curves posteriorly and slightly laterally away from the anterior edge of the orbit. The remainder of the zygomatic portion is missing from FMNH P14467 as well as from all but one of the other known *Pronothrotherium* skull specimens (Rovereto, 1914; Perea, 1988). Fragments of the zygomatic process are preserved in FMNH P14503 (Fig. 4 and Paula Couto, 1979: fig. 226). These indicate that a large descending process and a narrow ascending process were present. The ascending process bears a low, rounded postorbital process. However, the orientation of the ascending process as reconstructed by the original preparators of the specimen is conjectural. Indeed, they have reconstructed this process in a horizontal orientation as in *Paramylodon* (Stock, 1925) and some *Nothrotherium* specimens (Cartelle & Fonseca, 1983; Cartelle, 2012), rather than a more vertical orientation like that of other *Nothrotherium* material (Reinhardt, 1878), as well as *Mionothropus* (Frailey, 1986; De Iuliis *et al.*, 2011), *Nothrotheriops* (Stock, 1925), and *Hapalops* (Scott, 1903, 1904).

Frontal. The frontal is completely preserved on both the left and right sides, with the exception of a transverse plaster-filled crack extending across both sides just anterior to the

frontoparietal contact (Figs. 3.3, 7). The frontal contacts the nasal and the maxilla anteriorly on the dorsal surface of the snout (Fig. 7). It contacts the lacrimal, jugal, and maxilla anteroventrally within the orbit (Fig. 6). Posteriorly, the frontal has an interdigitated suture with the parietal located at the level of the foramen ovale, just behind the anterior edge of the glenoid fossa. Posteroventrally, it contacts the alisphenoid and orbitosphenoid (Fig. 6.3). The dorsal profile of the frontal is slightly convex anteroposteriorly in lateral view (Fig. 6), as in *Nothrotheriops* (Stock, 1925) but not *Nothrotherium* (Reinhardt, 1878; Paula Couto, 1971; Cartelle, 2012).

The postorbital process of the frontal is weak and rounded (Fig. 7). The temporal lines connected to the processes are also weak anteriorly. However, in the posterior half of the frontal, they form broad elevated ridges that converge posteriorly. The temporal lines in *Pronothrotherium* are more pronounced than those of *Nothrotheriops* (Stock, 1925) and *Nothrotherium* (Reinhardt, 1878; Cartelle, 2012), resembling the condition in *Mionothropus* (De Iuliis *et al.*, 2011) and *Hapalops* (Scott, 1903, 1904). A low sharp midline crest forms medial to the temporal lines beginning at the plaster-filled crack across the frontal and extending posteriorly to the frontoparietal suture itself (Figs. 3.3, 7). Because this crest is medial to the temporal lines, it is not the true sagittal crest, which is present more posteriorly on the parietal. However, based on the arrangement of muscles in the dog (Evans & Christensen, 1979) and in living tree sloths (Naples, 1985), and the presence of a similar crest in the extant armadillo *Euphractus* serving the same function (Wible & Gaudin, 2004), we suggest that this crest serves as the site of origin for superficial ear muscles (Evans & Christensen, 1979). No sagittal crest is present on either the frontal or parietal in *Nothrotheriops* (Stock, 1925), *Nothrotherium* (Cartelle, 2012), or *Mionothropus* (De Iuliis *et al.*, 2011). In *Hapalops* the development of the sagittal crest on the frontal and parietal varies among species (Scott, 1904: pl. 38). Based on our analysis of the computed tomography of the skull of *Pronothrotherium* FMNH 14467, the frontal appears as the most pneumatized cranial element (Fig. 8). The frontal sinuses originate anteriorly at the contact between the nasal and the frontal (Fig. 8.1–3) and taper posteriorly at the frontoparietal suture (Fig. 8.1–2). The frontal sinuses also largely extend ventrally and laterally, reaching their maximum expansion, in coronal section, at the level of the ala hypochiasmata (Fig. 8.4). The frontal sinuses of *Pronothrotherium* resemble those of extant *Bradypus variegatus* in being delimited posteriorly by the frontoparietal suture, whereas in other sloths such as the extant *Choloepus* and the extinct mylodontids *Catonyx* and *Glossotherium*, the frontal sinuses invade the parietal to some degree (Boscaini *et al.*, 2020a, 2020b).

A greatly reduced foramen for the frontal diploic vein (= supraorbital foramen; see Gaudin, 2004) is present on the dorsal surface of the right frontal just posterior to the postorbital process and lateral to the temporal line. This foramen appears to be absent on the left frontal. It is well developed in *Nothrotheriops* (Stock, 1925), *Mionothropus* (De Iuliis *et al.*, 2011), and *Hapalops* (Scott, 1903, 1904).

The orbital portion of the frontal is slightly concave anteroposteriorly in dorsal view. It forms a robust pointed orbital process lateral to the opening of the confluent optic foramen/sphenorbital fissure (Fig. 6). This process is likely the site of origin of the extrinsic eye muscles, and is almost certainly homologous with the ossified ala hypochiasmata of the orbitosphenoid identified in the extant armadillo *Euphractus* by Wible and Gaudin (2004), a process also found on the alisphenoid in the pampathere *Holmesina* (Gaudin & Lyon, 2017). This process is continuous on either side with an anterior inferior temporal crest and a posterior inferior temporal crest. The former is low and rounded for most of its length, extending anterodorsally across the frontal towards the postorbital process. The latter is sharper and more raised. It extends posteriorly along the alisphenofrontal contact, the crest extending onto the lateral surface of the squamosal and becoming confluent posteriorly with the anterior edge of the glenoid fossa. A frontal ala hypochiasmata connected to anterior and posterior infratemporal crests is also present in *Nothrotheriops* (Stock, 1925) and *Mionothropus* (De Iuliis *et al.*, 2011).

Parietal. The parietal is completely preserved on both left and right sides of the skull. It contacts the frontal anteriorly and the occipital posteriorly (Fig. 7). The occipitoparietal suture is located along the nuchal crest. It is V-shaped with the apex at the sagittal crest pointing anteriorly. Both descending sides of the V are concave anteriorly. The parietal

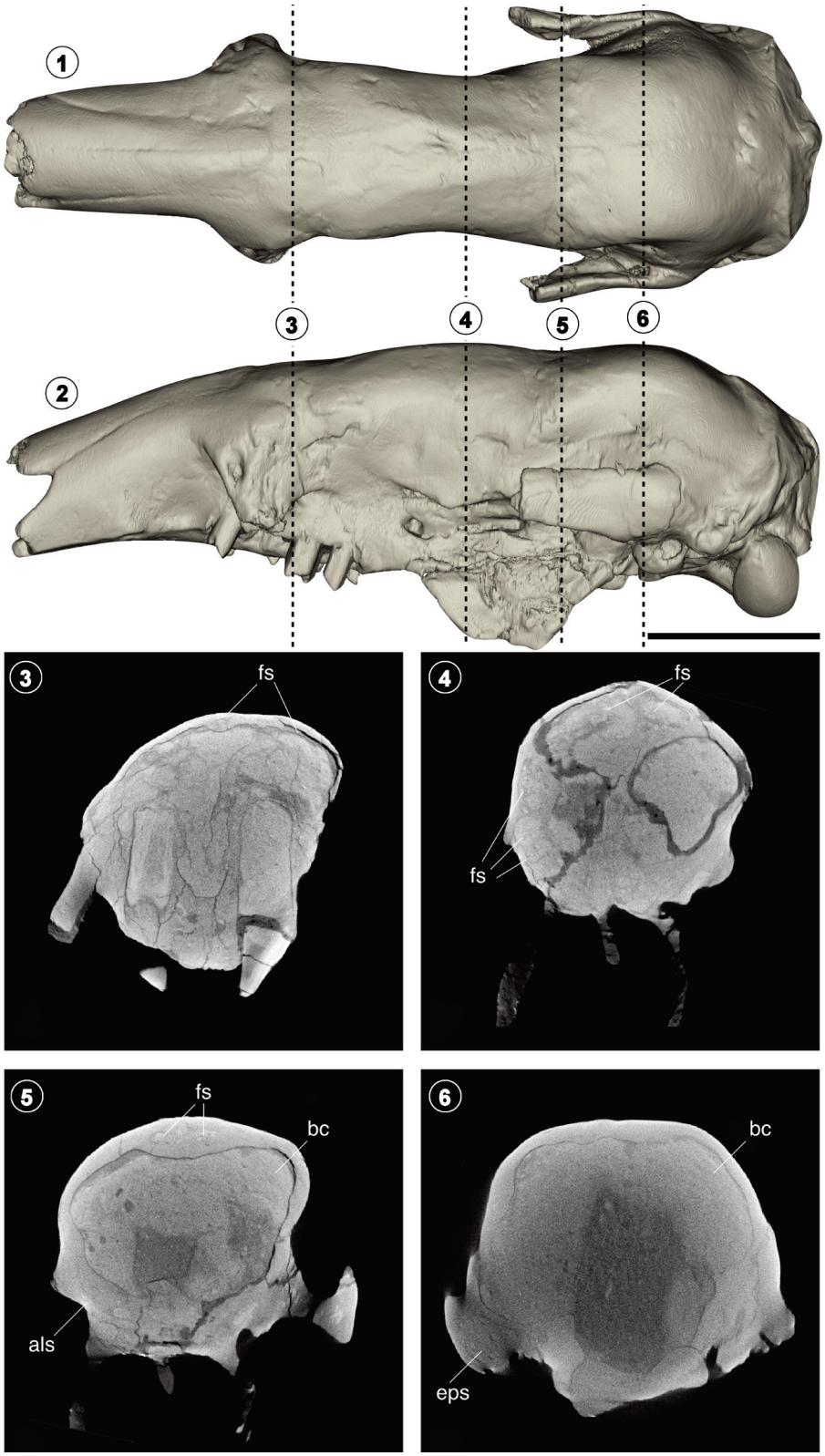

Figure 8. Skull of ***Pronothrotherium typicum***, **FMNH P14467**, showing 3-dimensional model based on CT-scanning in: **1,** dorsal view; **2,** left lateral view. Selected transverse sections from CT scan illustrated below: **3,** transverse section through Mf3 in anterior view; **4,** transverse section through frontal and ala hypochiasmata in anterior view; **5,** transverse section just behind frontoparietal suture in anterior view; **6,** transverse section through epitympanic sinus in anterior view. Abbreviations: **als,** alisphenoid; **bc,** brain cavity; **eps,** epitympanic sinus; **fs,** frontal sinus. Scale bar= 5 cm.

contacts the squamosal ventrally, forming a horizontal suture (Fig. 6). An elongated anteroventral process of the parietal extends between the frontal and squamosal, contacting the alisphenoid at its terminus. An alisphenoparietal contact is also present in *Nothrotherium* and variably present in *Nothrotheriops* and *Hapalops*, but is absent in *Mionothropus* (Gaudin, 2004; De Iuliis *et al.*, 2011).

The parietal is convex anteroposteriorly but flat transversely in its medial half, forming a distinct, hemicylindrical parietal eminence (Fig. 6). The lateral walls of the parietal are noticeably concave along the sidewalls of the temporal fossa. This concavity is absent in *Nothrotheriops* (Stock, 1925) and *Mionothropus* (De Iuliis *et al.*, 2011), but is sometimes present in *Hapalops* (Scott, 1903, 1904). The parietal eminence in *Pronothrotherium* is the highest point on the cranium. This condition is similar to that in *Hapalops* (Scott, 1903, 1904) and *Nothrotherium* (Reinhardt, 1878; Cartelle & Fonseca, 1983; Cartelle, 2012). However, a parietal eminence is absent in *Nothrotheriops* (Stock, 1925) and *Mionothropus* (Frailey, 1986; De Iuliis *et al.*, 2011), where the frontal forms the highest point on the skull.

The parietal bears a low rounded sagittal crest along its mid-dorsal surface (Fig. 7). Nearly the entire dorsal surface of the parietal eminence is covered by numerous shallow, transversely oriented muscle scars produced by the temporalis muscle. The scarring extends posteriorly to the nuchal crest, suggesting that the temporalis originates at the nuchal crest. This stands in contrast to the condition in other nothrotheriids (Reinhardt, 1878; Stock, 1925; Cartelle & Fonseca, 1983; Frailey, 1986; De Iuliis *et al.*, 2011), in which the crest marking the posterior limit of the temporal fossa lies well anterior to the nuchal crest. The latter is a feature that evolves convergently in a wide variety of sloth taxa (Gaudin, 2004).

Squamosal. The squamosal is almost completely preserved on both sides (Figs. 5–7). However, on the left side the anterior tip of the zygomatic process is missing, and there are plaster-filled cracks medial and posterior to the glenoid fossa on this side as well (Fig. 6). The squamosal contacts the alisphenoid, pterygoid, ectotympanic, and petrosal ventrally and medially. It contacts the mastoid exposure of the petrosal posteroventrally and the parietal dorsally. A small posterodorsal contact occurs between the squamosal and occipital on the left side of the skull, but it is absent on the right.

In the specimen of *Pronothrotherium* illustrated in Figure 6 (FMNH P14467), the zygomatic process of the squamosal is deeper and shorter than the elongated, narrow process of *Nothrotheriops* (Stock, 1925). The zygomatic process of FMNH P14503 (Fig. 4 and Paula Couto, 1979, fig.: 226), though incomplete anteriorly, is even deeper than that of FMNH P14467. The relative length of the zygomatic process in *Pronothrotherium* (45.0 mm, 17% of CML —based on FMNH P14467) is intermediate between that of *Hapalops brachycephalus* (35.1 mm, 13% of CML —based on AMNH 9176) and *Nothrotheriops shastensis* (68.1 mm, 26% of CML —based on the cast LACMHC 1800-3). The process extends anteriorly to the level of the ala hypochiasmata of the frontal (Fig. 6.3), as in *Mionothropus* (De Iuliis *et al.*, 2011), whereas in *Nothrotheriops* the process extends beyond the ala anteriorly. The zygomatic process is oriented anteroposteriorly (Figs. 5, 7) as in other nothrotheriids (Frailey, 1986; Gaudin, 1995, 2004; McDonald & Muizon, 2002; De Iuliis *et al.*, 2011), and tapers anteriorly in lateral view, forming a rounded tip at its end.

The zygomatic process of the squamosal bears a large lateral inflation at the root of the zygoma (Fig. 5), also found in *Nothrotheriops* (Stock, 1925), *Nothrotherium* (Guth, 1961), and *Hapalops*, but not *Mionothropus* (De Iuliis *et al.*, 2011). This bulge accommodates the epitympanic sinus (Fig. 8.4), a dorsal extension of the tympanic cavity into the squamosal that is typical for megatherioid sloths, whereas mylodontid sloths feature a shallow epitympanic recess in this area. The squamosal forms the anterior and lateral walls of the sinus (Patterson *et al.*, 1992). The lateral surface of the zygomatic process becomes slightly concave in front of the "epitympanic bulge" before flattening anteriorly. The area immediately posterior to the bulge is also concave anteroposteriorly, presumably forming a superficies meatus to accommodate the cartilaginous external auditory canal. Behind this is a large, bulbous process termed a "mastoid process" by Patterson *et al.* (1992). This is likely formed mostly by the paroccipital process of the petrosal (Wible & Gaudin, 2004; Gaudin, 2011), with an anterior contribution from the posttympanic process of the squamosal, as in other sloths, though the two bones are fused in this

region in typical sloth fashion (Boscaini et al., 2018b). As in other nothrotheriids and in contrast to the condition in other sloths (Gaudin, 1995), the canal for the occipital artery perforates the posterior margin of this "mastoid process", with the posttemporal foramen located just posterior and dorsal to the process (Fig. 6).

A deep pocket of the temporal fossa covers the entire dorsomedial surface of the zygomatic process (Fig. 7). A sharp crest extends along the dorsolateral edge of the process, marking the lateral edge of the temporal fossa. In *Pronothrotherium*, this crest ends abruptly over the lateral inflation described above, whereas in other nothrotheriids (Reinhardt, 1878; Stock, 1925; Cartelle & Fonseca, 1983; Frailey, 1986; De Iuliis *et al.*, 2011), this crest continues posterodorsally across the braincase, connecting to the temporal lines of the parietal.

The glenoid fossa lies on the ventromedial surface of the zygomatic process (Figs. 3.4, 5). The U-shaped fossa is concave both transversely and anteroposteriorly and has a slight anterodorsal incline. The fossa is widest anteriorly and is bounded posteromedially by a slightly raised, rounded entoglenoid process. In *Pronothrotherium*, the surface of the postglenoid region is rugose, differing from that of *Nothrotheriops* (Stock, 1925; Gaudin, 1995) and *Mionothropus* (De Iuliis *et al.*, 2011), where this region is traversed by longitudinal grooves. A few small vascular openings occur in the postglenoid region. One of these may represent a reduced postglenoid foramen (Patterson *et al.*, 1992; Gaudin, 1995).

Occiput. The occiput is well-preserved. However, the ventral end of the external occipital crest is reconstructed in plaster (see below), and a perforation is present on the right side of the exoccipital region below the ventral nuchal crest (Fig. 9). Anterodorsally, the occiput contacts the parietal almost exclusively, the sole exception being the small connection with the squamosal on the left side mentioned previously. The occipital contacts the mastoid and entotympanic anteroventrally.

As in all nothrotheriids (Gaudin, 2004), the supraoccipital is well-exposed on the dorsal surface of the skull (Fig. 7). This dorsal exposure is raised above the level of the parietal, as in *Mionothropus* (De Iuliis *et al.*, 2011) and unlike *Nothrotheriops* (Stock, 1925) and *Hapalops* (Scott, 1903, 1904), where it is level with the parietal. The supraoccipital bears a short, weak midline crest on its dorsal surface (Fig. 9), in contrast to the prominent crest present in *Nothrotheriops* (Stock, 1925). The surface of the dorsal supraoccipital exposure is moderately rugose in *Pronothrotherium* and very rugose in *Nothrotheriops* (Stock, 1925). It is presumably the site of attachment for the occipitalis muscle or caudal dor-

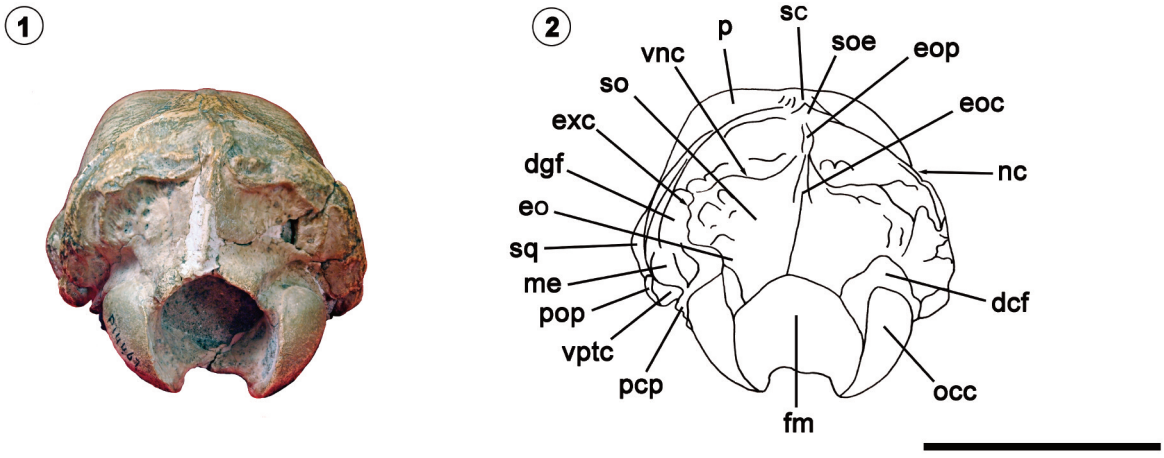

Figure 9. Skull of ***Pronothrotherium typicum*, FMNH P14467**, in posterior view. **1,** photograph of skull. **2,** labeled drawing. Abbreviations: **dcf,** dorsal condyloid fossa; **dgf,** digastric fossa; **eo,** exoccipital; **eoc,** external occipital crest; **eop,** exoccipital protuberance; **exc,** exoccipital crest; **fm,** foramen magnum; **me,** mastoid exposure of petrosal; **nc,** nuchal crest; **p,** parietal; **pcp,** paracondylar process; **pop,** paroccipital process of petrosal (= mastoid process of Patterson *et al.* 1992); **occ,** occipital condyle; **sc,** sagittal crest; **so,** supraoccipital; **soe,** dorsal supraoccipital exposure; **sq,** squamosal; **vnc,** ventral nuchal crest; **vptc,** ventral entrance to posttemporal canal/opening to canal for occipital artery. Scale bar= 5 cm.

sal ear muscles, which attach in this region in living sloths (Naples, 1985) and in the dog (Evans & Christensen, 1979).

The nuchal crest of *Pronothrotherium* is much more prominent than that of *Nothrotheriops* (Stock, 1925). However, both possess a strong, transversely oriented, ventral nuchal crest (Fig. 9). This condition is apparently common to all nothrotheriids (Reinhardt, 1878; Stock, 1925; Cartelle & Fonseca, 1983; Frailey, 1986; De Iuliis *et al.*, 2011) and certain other sloths (*e.g.*, *Eucholoeops*, *Hapalops*, *Analcimorphus*, Megatheriidae, Megalonychidae; Gaudin, 2004). Presumably, the more dorsal nuchal crest serves as the point of insertion for superficial neck muscles (*e.g.*, *splenius*, *obliquus capitis*; Evans & Christensen, 1979), whereas the ventral nuchal crest serves as the point of insertion for deep neck muscles, as seen in the dog (*e.g.*, *rectus capitis dorsalis*; Evans & Christensen, 1979), as also inferred for *Hapalops* by Naples and McAfee (2014). The dorsal and ventral nuchal crests meet laterally (Fig. 6). Medial to this confluence, a vertical exoccipital crest (Gaudin, 1995) extends ventrally from the ventral nuchal crest. In *Pronothrotherium*, this crest ends abruptly at a level dorsal to the occipital condyles, unlike *Nothrotheriops* (Stock, 1925), where the exoccipital crest is continuous ventrally with the paracondylar process. The ventral nuchal crest and exoccipital crest outline a large rugose digastric fossa on the posterior surface of the occipital in both *Pronothrotherium* (Fig. 9) and *Nothrotheriops* (Stock, 1925).

The external occipital protuberance is large and bulbous in *Pronothrotherium* and lies at the midpoint of the ventral nuchal crest (Figs. 7, 9), as it does in *Mionothropus* (De Iuliis *et al.*, 2011). This location is unusual and stands in contrast to the condition in *Nothrotheriops* (Stock, 1925) and in other mammals (*e.g.*, Pick & Howden, 1977; Evans & Christensen, 1979), where the protuberance is more anteriorly and dorsally located, just posterior to the midpoint of the dorsal nuchal crest. The external occipital crest descends ventrally from the external occipital protuberance. However, its length cannot be determined due to damage in this area. The midline of the occiput has been reconstructed in plaster from a point 10 mm below the external occipital protuberance to the dorsal rim of the foramen magnum (Fig. 9).

In ventral view, the smooth, convex occipital condyles are somewhat compressed anteroposteriorly, their transverse width exceeding their anteroposterior length (Figs. 3.4, 5). In posterior view, they are elongated dorsoventrally, their dorsoventral length much greater than their transverse width (Fig. 9). Above the dorsal edge of the condyle in *Pronothrotherium*, there is a well-marked depression, the dorsal condyloid fossa. In *Nothrotheriops* (Stock, 1925), this fossa is narrower but bears a distinct condyloid canal lacking in *Pronothrotherium*. The exoccipital region is marked by a weak paracondylar process extending below the ventrolateral edge of the condyle. The paracondylar process appears to be intact on the right side but is damaged on the left (Fig. 3.4). This process is similar in size to that of *Hapalops* (Gaudin, 1995); it is much less robust than that of *Nothrotheriops* (Stock, 1925; Gaudin, 1995) or *Mionothropus* (De Iuliis *et al.*, 2011). The hypoglossal foramen lies below the ventromedial edge of the condyle (Fig. 5). The hypoglossal foramen in *Pronothrotherium* is ventral to the jugular foramen, whereas in *Nothrotheriops* (Stock, 1925), the hypoglossal foramen is recessed dorsally and thus lies at the same level as the jugular foramen. In *Mionothropus*, it is situated in an intermediate position (De Iuliis *et al.*, 2011).

The large foramen magnum is round in *Pronothrotherium* (Fig. 9), in contrast to the slightly oval foramen in *Nothrotheriops* (Stock, 1925). The dorsal rim of the foramen is indented dorsally in the midline and flanked on either side by posteriorly projecting lappets with rounded edges, as in other nothrotheriids (Reinhardt, 1878; Stock, 1925; Cartelle & Fonseca, 1983; Frailey, 1986; De Iuliis *et al.*, 2011). *Pronothrotherium* further resembles *Nothrotheriops* (Stock, 1925) and other nothrotheriids (Reinhardt, 1878; Cartelle & Fonseca, 1983; Frailey, 1986; De Iuliis *et al.*, 2011) in that the foramen magnum and occipital condyles are directed posteroventrally.

Edmund (1985) noted that the foramen magnum and occipital condyles are directed in a similar posteroventral orientation in living armadillos and correlated this condition with a posture where the head is carried in a nose-down position. This author inferred a similar head orientation for extinct pampatheres, which share with extant armadillos a posteroventral orientation of the foramen magnum and occipital condyles. We note that in such a nose-down position, the dorsal-most portion of the head may lie behind the nuchal crest, over the ventral nuchal crest. This may in turn

place additional strain on deep neck muscles, and require an augmentation of their role in holding up the head. Therefore, the presence of an enlarged ventral nuchal crest, to which these deep neck muscles attach, coupled with the orientation of the foramen magnum and occipital condyles, strongly supports a nose-down orientation of the head in nothrotheriids.

Basioccipital. The basioccipital is completely preserved. It is sutured to the basisphenoid anteriorly and fused to the occipital posterolaterally. It abuts the entotympanic anterolaterally. In FMNH P14467, the basioccipital is shaped like the top of an hourglass, with wide, rounded lateral extensions anteriorly and a strong constriction posteriorly (Fig. 5). The rounded lateral extensions are formed by large anterior basioccipital tubera. Immediately posterior to the tubera are a pair of rather small but deep depressions for the *rectus capitis ventralis* muscles (Evans & Christensen, 1979). The basioccipital in FMNH P14503 (Fig. 4.2) is remarkably different from that of FMNH P14467 (Figs. 3.4, 5). It is much wider transversely than that of FMNH P14467, and the depressions it bears for the rectus *capitis ventralis* muscles are much larger, forming wide, shallow fossae separated by a median keel (Fig. 4.2). The basioccipital tubera are also absent in FMNH P14503. In other nothrotheriids (Reinhardt, 1878; Stock, 1925; Guth, 1961; De Iuliis *et al.*, 2011), the basioccipital is shorter anteroposteriorly and does not taper as much posteriorly as that of FMNH P14467. However, these other nothrotheriids resemble FMNH P14467 in their possession of large anterior basioccipital tubera. Also, *rectus capitis* fossae are present in *Nothrotheriops* (Stock, 1925) and *Mionothropus* (De Iuliis *et al.*, 2011). In the former taxon, they are quite small and shallow, whereas in the latter taxon they are both larger and deeper than those of FMNH P14467, resembling instead FMNH P14503, with its large fossae separated by a median keel.

Basisphenoid. The basisphenoid is also completely preserved. It is a flat, triangular bone that contacts the basioccipital posteriorly and is overlapped anteromedially by the vomer and anterolaterally by the pterygoid (Fig. 5). The left posterior corner of the basisphenoid forms a narrow lappet that ascends between the basioccipital and the pterygoid into the medial wall of the carotid canal.

Vomer. The enlarged vomer is well preserved and broadly exposed in the roof of the nasopharynx (Fig. 5). The portion within the nasal cavity is obscured by matrix, as are parts of the vomerine wings just posterior to the choanae. The right wing of the vomer is perforated by two holes. The perforations show that the vomerine wings are composed of a very thin layer of bone, as is the case in *Nothrotheriops* (Gaudin, personal observation). As described below, the vomer bears a large longitudinal crest. This crest is completely preserved anteriorly and posteriorly, but a small piece of the crest is missing anterior to its bulbous posterior expansion.

As noted by Patterson *et al.* (1992: page 27), the vomer is "an extraordinary bone" in *Nothrotheriops*, a description that can be aptly applied to *Pronothrotherium* and the other nothrotheriids as well (Guth, 1961; Gaudin, 2004; De Iuliis *et al.*, 2011). In all nothrotheriid taxa, the vomerine wings are greatly expanded posteriorly, forming the bulk of the nasopharyngeal roof and covering the presphenoid and anterior portions of the basisphenoid. The wings are sutured to the palatine and pterygoid laterally, the latter contact accounting for the posterior two-thirds of the suture. The vomerine wings appear to have a small sutural contact with the basisphenoid posteriorly.

The vomer bears a remarkable ventral, asymmetrical longitudinal crest in all undoubted nothrotheriids. The crest is straight but offset to the left anteriorly in *Pronothrotherium* (Fig. 5), whereas in *Mionothropus* it is straight but offset to the right (De Iuliis *et al.*, 2011), and in *Nothrotherium* (Reinhardt, 1878; Paula Couto, 1980) and *Nothrotheriops* (Lull, 1929; Patterson *et al.*, 1992; see also Stock, 1925: fig. 10A), it is curved, beginning anteriorly left of the midline, and curving widely to the right and then back to the left posteriorly. The ventral edge of the crest in *Pronothrotherium* curls laterally to the left so that the right lateral surface of the crest is convex dorsoventrally whereas the left lateral surface of the crest is concave dorsoventrally, in contrast to the vertical crest present in *Mionothropus* (De Iuliis *et al.*, 2011). The depth of the crest in *Pronothrotherium* is roughly two-thirds the depth of the choanae, making it much deeper and thicker than the low, thin crest in *Nothrotheriops* (Lull, 1929; Patterson *et al.*, 1992; also based on the cast of LACMHC 1800-3), though less tall than that of *Mionothropus* (De Iuliis *et al.*, 2011). Posteriorly the

vomerine crest of FMNH P14467 bears a large bulbous expansion, which curves slightly left of the midline and overlaps ventrally but does not contact the basisphenoid, a feature not observed in other nothrotheriids. A pronounced, asymmetrical vomerine crest is not present in any sloth outside the Nothrotheriidae (*sensu* Gaudin, 2004), and indeed, we are unaware of a similar structure in any mammal.

Pterygoid. The ventral portion of the pterygoid is poorly preserved on both sides of the skull. The descending lamina is composed of fragments of bone held together by a substantial amount of plaster on the left (Figs. 3.1, 6). On the right side this area is completely reconstructed in plaster (Figs. 3.2, 6). The bone fragments on the left preserve enough of the natural edge of the descending lamina to be confident in its shape. The orbital portion of the pterygoid is broken in several places on the right, but is better preserved on the left. Its dorsal suture is damaged on both sides in the vicinity of the foramen rotundum. The nasopharyngeal portion of the pterygoid is well preserved on both sides (Fig. 5).

The orbital portion of the pterygoid is sutured to the palatine anteriorly and the alisphenoid and squamosal dorsally (Fig. 6). The pterygoid does not participate in the foramen ovale, but contacts the squamosal immediately posterior to it (Fig. 6.2–6.3). This squamosopterygoid suture extends posteriorly into the tympanic cavity. The pterygoid may have a small participation in the anteroventral rim of the foramen rotundum; however, this is difficult to determine because the precise position of the alisphenopalatine and palatopterygoid sutures are unclear in this area. Like *Mionothropus* (De Iuliis *et al.*, 2011), the pterygoid has a large exposure in the lateral wall and roof of the nasopharynx (Fig. 5), where it contacts the palatine anteriorly, the vomer anteromedially, and the basisphenoid posteromedially. This portion of the pterygoid is deeply excavated medially, though not quite so much as in *Mionothropus* (De Iuliis *et al.*, 2011). As in the latter, this may have accommodated a soft walled cavity representing a structural precursor to the large osseous pterygoid bullae of the Pleistocene nothrotheriids *Nothrotherium* (Reinhardt, 1878; Cartelle & Fonseca, 1983) and *Nothrotheriops* (Stock, 1925).

The descending lamina of the pterygoid does not extend as far ventrally as that in *Nothrotheriops* (Stock, 1925). The ventral edge of the lamina is flat, with squared-off corners. This contrasts with the semicircular edge common to other nothrotheriids (Stock, 1925; Cartelle & Fonseca, 1983; Frailey, 1986; De Iuliis *et al.*, 2011), and indeed other sloths (Gaudin, 2004). On the posterior edge of the lamina there is a groove for the *tensor veli palatini* muscle (Figs. 5–6). This groove is present in other sloth taxa (Patterson *et al.*, 1992; Gaudin, 1995). Immediately posterior to the dorsal end of this groove is a shorter, shallower groove that accommodated the eustachian tube.

Alisphenoid. The alisphenoid is well preserved. However, on the left side of the skull, its ventral suture with the pterygoid is damaged along the ventral rim of the foramen rotundum. On the right side, a plaster-filled crack is present on the posterolateral rim of the foramen ovale. The alisphenoid lies in the center of the medial orbital wall, contacting the palatine and orbitosphenoid anteriorly, the frontal anterodorsally, the squamosal posterodorsally, and the pterygoid ventrally (Fig. 6).

In its posterior region, the alisphenoid surrounds the foramen ovale both internally and externally. This condition differs from *Nothrotheriops* (Stock, 1925), *Hapalops* (Scott, 1903, 1904), and most other sloths (*e.g.*, other basal megatherioids, extant *Bradypus*, and *Choloepus*, as well as Mylodontidae, Megatheriidae, and *Megalonyx*; Gaudin *et al.*, 1996; Gaudin, 2004) in which the pterygoid and/or squamosal form portions of the external rim of the foramen. Anterodorsally the alisphenoid forms the dorsal and posteroventral rim of the foramen rotundum and its medial wall (Fig. 6.2–6.3). It is unclear whether the anteroventral rim of the foramen rotundum is formed by the pterygoid, palatine, or alisphenoid. The alisphenoid also forms the posterior wall of the sphenorbital fissure/optic foramen, as it does in *Mionothropus* (De Iuliis *et al.*, 2011) and *Nothrotheriops* (LACMHC 1800-4, 1800-6).

Orbitosphenoid. A tiny surface exposure of orbitosphenoid is preserved in the orbit on both sides of the skull. This orbital exposure contacts the frontal anterodorsally, the palatine ventrally, and the alisphenoid posteriorly (Fig. 6). The orbitosphenoid forms the medial wall of the fused sphenorbital fissure/optic foramen. It contributes to the posterior roof and floor of the groove that emerges ante-

riorly from the sphenorbital fissure/optic foramen (and continues anteriorly across the frontal). In both *Mionothropus* (De Iuliis *et al.*, 2011) and *Nothrotheriops* (LACMHC 1800-4, 1800-6), the orbitosphenoid also contributes to the dorsal margin of the sphenorbital fissure/optic foramen. The opening of the optic foramen remains covered by matrix in *Pronothrotherium*, but must have been deeply recessed within the combined opening of the sphenorbital fissure/optic foramen.

Mandible

The mandible of FMNH P14467 was not preserved, and only a small portion of the horizontal ramus is preserved in FMNH P14503 (Paula Couto, 1979: fig. 226). However, an isolated mandible, FMNH P14350, is available (Fig. 10). The specimen is relatively well preserved and is indeed the only known specimen of *Pronothrotherium* in which the ascending ramus is preserved. The left side of the mandible is better preserved than the right. It includes large portions of the coronoid, condyloid, and angular processes, although distal pieces of each process are missing. The anterior region of the mandible is broken dorsally and ventrally, with the anterior end of the mandibular spout missing entirely. It is reconstructed in Figure 10 based on the type specimen (Rovereto, 1914), which is more complete anteriorly and bears an elongated, narrow spout.

The horizontal ramus of the mandible resembles that of *Hapalops* (Scott, 1903, 1904) and *Mionothropus* (De Iuliis *et al.*, 2011). It is more slender than that of *Nothrotheriops* (Stock, 1925), *Lakukullus* (Pujos *et al.*, 2014), and *Aymaratherium* (Pujos *et al.*, 2016), with a less pronounced ventral bulge accommodating the molariforms, though the ventral bulge is more pronounced than in *Nothrotherium* (Reinhardt, 1878; Cartelle & Fonseca, 1983; Cartelle, 2012). A second, smaller

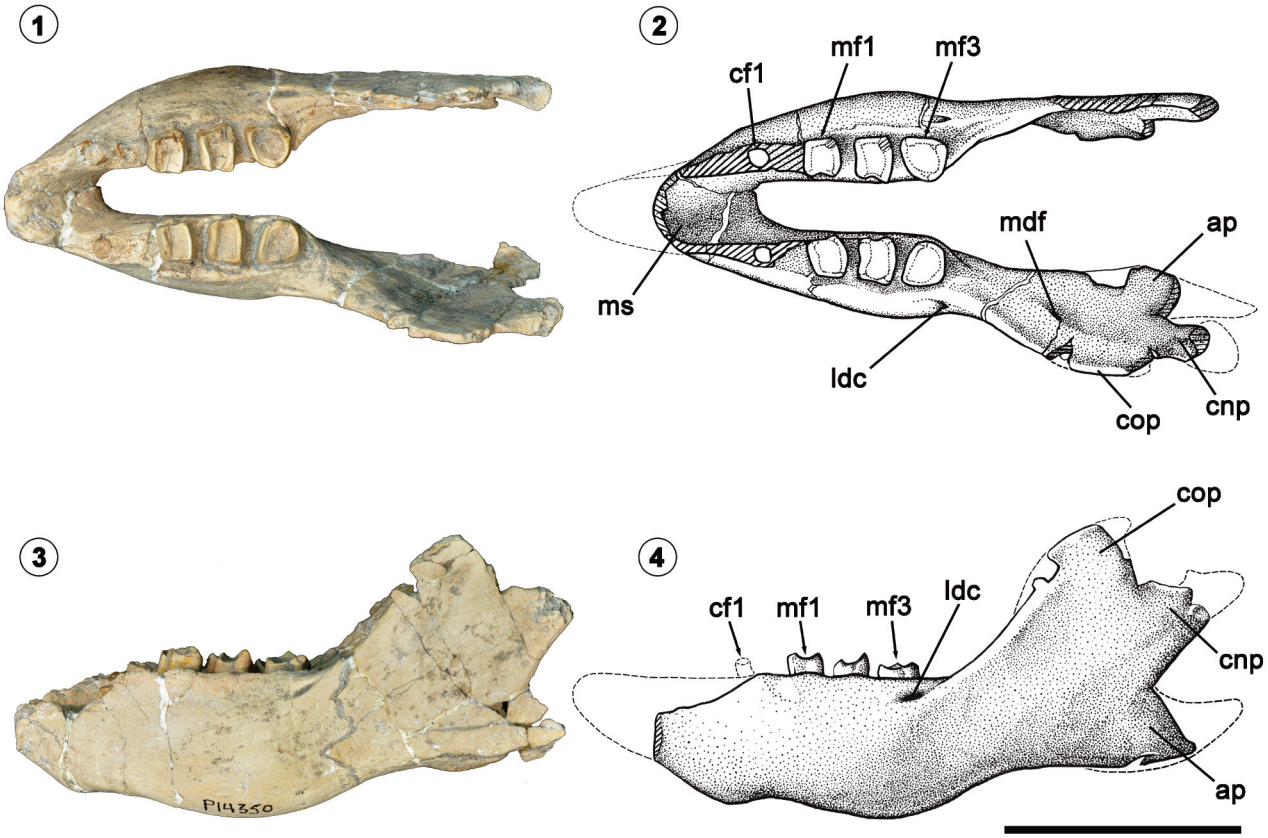

Figure 10. Mandible of ***Pronothrotherium typicum*, FMNH P14350**. **1,** occlusal view, photograph. **2,** occlusal view, labeled drawing. **3,** left lateral view, photograph. **4,** left lateral view, labeled drawing. Abbreviations: **ap,** angular process; **cf1,** lower caniniform; **cnp,** condyloid process; **cop,** coronoid process; **ldc,** lateral dentary canal; **mf1/3,** lower first/third molariform; **mdf,** mandibular foramen; **ms,** mandibular symphysis. Scale bar= 5 cm.

and more anterior bulge is present marking the angle at which the symphysis joins the ventral edge of the horizontal ramus. This angle is present only in juvenile *Nothrotheriops* (Naples, 1990), though it is found in *Hapalops* (Scott, 1903, 1904) and in *Mionothropus* (De Iuliis *et al.*, 2011), *Nothropus priscus* (Burmeister, 1882), and *Nothrotherium* (Reinhardt, 1878; Cartelle & Fonseca, 1983; Cartelle, 2012).

The coronoid, condyloid, and angular processes are positioned equidistant from each other, resembling *Halalops* (Scott, 1903, 1904) and *Mionothropus* (Frailey, 1986; De Iuliis *et al.* 2011) but differing from *Nothrotheriops* (Stock, 1925) and *Nothrotherium* (Cartelle & Fonseca, 1983), where the coronoid and condyloid processes are closer to each other than to the angular process and the condyle is farther elevated above the tooth row. The coronoid process is slightly lower than that of *Mionothropus* (Frailey, 1986; De Iuliis *et al.*, 2011) and *Nothrotherium* (Cartelle & Fonseca, 1983) and much lower than that of *Nothrotheriops* (Stock, 1925) and *Hapalops* (Scott, 1903, 1904). The process is broader than that of *Mionothropus* (Frailey, 1986; De Iuliis *et al.*, 2011), *Nothrotheriops* (Stock, 1925), and *Hapalops* (Scott, 1903, 1904), resembling in this respect the coronoid of *Nothrotherium* (Cartelle & Fonseca, 1983). The anterior edge of the coronoid process is convex. Its posterior edge is not preserved.

The condyloid process is triangular as in other nothrotheriids (Stock, 1925; Cartelle & Fonseca, 1983; Frailey, 1986; De Iuliis *et al.*, 2011) except *Aymaratherium* (Pujos *et al.*, 2016). However, its length in *Pronothrotherium* cannot be measured because the entire condyle is missing.

The shape of the angular process is impossible to determine; its ventral edge is distorted and its dorsal edge and distal end are missing. It is reconstructed based on the preserved angular process of *Nothrotheriops* (Wilson, 1942). Enough of the angular process is preserved to show that it was much deeper than that of *Hapalops* (Scott, 1903, 1904) and *Mionothropus* (Frailey, 1986; De Iuliis *et al.*, 2011), resembling the specimens of *Nothrotheriops* described by Lull (1929) and Wilson (1942). The angular process in the specimen of *Nothrotheriops* described by Stock (1925) is unusually narrow, perhaps due to postmortem distortion, though the angular process is also rather shallow in *Nothrotherium* (Cartelle & Fonseca, 1983; Cartelle, 2012) and *Lakukullus* (Pujos *et al.*, 2014). On the medial surface of the angular process there is a large depression to accommodate the medial pterygoid muscle. This depression is present in all sloths (Gaudin, 2004).

In occlusal view (Fig. 10), the posterior edge of the symphysis of FMNH P14350 lies anterior to cf1. This contrasts with the condition in the type specimen (Rovereto, 1914), in which the symphysis ends posterior to cf1, but resembles the condition in both *Pronothrotherium mirabilis* and *P. figueirasi* (Perea, 1988). FMNH P14350 also resembles both *Mionothropus* (Frailey, 1986; De Iuliis *et al.*, 2011) and *Hapalops* (Scott, 1903, 1904) in this respect.

A single lateral dentary canal (= posterior external opening of the mandibular canal —Engelmann, 1985; De Iuliis, 1994) is present on the lateral surface of the horizontal ramus, a condition characteristic of the Nothrotheriidae with the exception of some specimens of *Nothropus* (De Iuliis, 1994). The canal is situated lateral to the distal crest of mf3, as it is in *Pronothrotherium mirabilis* and *P. figueirasi* (Perea, 1988) and most other nothrotheriids (Stock, 1925; Lull, 1929; Cartelle & Fonseca, 1983; Pujos *et al.*, 2014). This opening lies posterior to mf3 in *Hapalops* (Scott, 1903, 1904) and *Aymaratherium* (Pujos *et al.*, 2016). Its position is variable in *Nothropus*. In *Nothropus priscus* (Burmeister, 1882), the lateral dentary canal is positioned posterior to mf3, whereas in *N. tarijensis* (Ameghino, 1907) the canal is lateral to mf3.

Lower dentition. As noted previously in regard to the upper dentition, *Pronothrotherium* differs from *Nothrotheriops* (Stock, 1925), *Nothrotherium* (Reinhardt, 1878; Cartelle & Fonseca, 1983), as well as *Nothropus carcaranensis* (Brandoni & McDonald, 2015), but resembles *Hapalops* (Scott, 1903, 1904), *Nothropus priscus* (Burmeister, 1882), *N. tarijensis* (Ameghino, 1907), *Mionothropus* (Frailey, 1986; De Iuliis *et al.*, 2011), *Lakukullus* (Pujos *et al.*, 2014), and *Aymaratherium* (Pujos *et al.*, 2016), in its retention of a small lower caniniform. The length of the tooth row in FMNH P14350 (45 mm) is intermediate between *Pronothrotherium mirabilis* (39.7 mm —Perea, 1988) and the type specimen (>50 and <58 mm —based on measurements by Rovereto, 1914). Perea (1988, p. 382) stated that *P. figueirasi* is "*Tamaño comparable a* Pronothrotherium mirabilis." (Of a size comparable to that of *Pronothrotherium mirabilis*).

Only the alveolus of the right cf1 is preserved; the left cf1 is missing entirely. The left mf1 and mf2 and the left and right mf3 are well preserved. The occlusal surfaces of the right mf1 and mf2 are damaged, bearing breaks on their distolabial corners.

Based on the preserved alveolus of cf1, the caniniform tooth is circular in cross-section. The caniniform is similar in size (4 mm, 9% of tooth row length) to that of *Mionothropus* (6 mm, 11% of tooth row length —Frailey, 1986; De Iuliis *et al.*, 2011) and *Nothropus priscus* (3.8 mm, 6.7% of tooth row length —TJG, unpubl. obs.), but smaller than that of *Hapalops* (8 mm, 17% of tooth row length —Scott, 1903, 1904). It is separated by a short diastema from the molariforms, as in *Mionothropus* (Frailey, 1986; De Iuliis *et al.*, 2011), *Nothropus* (Burmeister, 1882; Ameghino, 1907), and *Lakukullus* (Pujos *et al.*, 2014), and in contrast to *Aymaratherium* (Pujos *et al.*, 2016), which lacks this diastema.

In general shape the first two molariforms resemble those of *Nothrotheriops* (Stock, 1925) and other nothrotheriids (Burmeister, 1882; Ameghino, 1907; Cartelle & Fonseca, 1983; Frailey, 1986; De Iuliis *et al.*, 2011; Pujos *et al.*, 2014; but see unusual morphology in *Aymaratherium*, Pujos *et al.* 2016). Both mf1 and mf2 are quadrate, compressed mesiodistally; mf1 is slightly smaller than mf2. In occlusal view (Fig. 10), the mesial crest of mf1 is planar whereas the mesial crest of mf2 is concave anteriorly. The distal crest is convex posteriorly in occlusal view and higher than the mesial crest in both mf1 and mf2. A labial and lingual crest, both concave anteroposteriorly, connect the mesial and distal crests of mf1 and mf2, enclosing a basin of softer, modified orthodentine as in the upper dentition (Ferigolo, 1985; Kalthoff, 2011). In both mf1 and mf2 the labial surface bears a marked apicobasal sulcus, whereas the sulcus on the lingual surface is shallow. McDonald and Muizon (2002) assert that the presence of sulci is a character of nothrotheriids but is absent in *Hapalops*. However, Scott (1903, 1904; also Gaudin, pers. obs.) described weakly developed sulci in some specimens of *Hapalops* (see also Bargo *et al.*, 2019). The third molariform takes on a rounded triangular (almost circular) shape in occlusal view, with rounded sides and three prominent cusps. The rounded triangular shape of mf3 in FMNH P14350 differs from the other described specimens of *Pronothrotherium* (Rovereto, 1914; Perea, 1988) in which mf3 is more quadrate. It is reminiscent of the nearly circular mf3 in *Hapalops* (Scott, 1904: pl. 62, fig. 3), *Nothrotherium* (Cartelle & Fonseca, 1983), and *Nothropus priscus* (Burmeister, 1882; Ameghino, 1907). In *Nothrotheriops* (Stock, 1925; Lull, 1929), mf3 ranges from quadrate to circular, whereas it is quadrate in *Mionothropus* (Frailey, 1986; De Iuliis *et al.* 2011) and *Lakukullus* (Pujos *et al.*, 2014), and exhibits an unusual trapezoidal morphology in *Aymaratherium* (Pujos *et al.*, 2016). In lateral view, a labial crest connects the mesial and distal crests of mf3 in FMNH P14350. However, on the lingual side the mesial and distal crests meet to form a singular lingual cusp.

DISCUSSION

The genus *Pronothrotherium* currently contains three species, *P. typicum* (the type species), *P. mirabilis*, and *P. figueirasi,* the latter erected by Perea (1988). *Pronothrotherium figueirasi* is based only on one specimen (the type), an isolated left partial mandible, lacking even a complete lower dentition, but is distinctive, according to Perea (1988), primarily because it is smaller than *P. typicum* and younger than *P. mirabilis*, but also because it shares with *P. mirabilis* some relatively minor morphological differences from *P. typicum* (*e.g.*, more curved ventral border, more gracile overall form, somewhat narrower molariforms). De Iuliis (2018) has discussed the problems with basing new taxa on such scant evidence. Additionally, we believe that morphological evidence is required for differentiating species, *i.e.*, that minor temporal differences are themselves insufficient. Given these issues, we do not believe that *P. figueirasi* should be accepted as a valid taxon. Based on the available evidence, the scant remains of *P. figueirasi* are not distinguishable morphologically or metrically from those of *P. mirabilis*, and so we consider the former a synonym of the latter.

The case for the validity of *P. mirabilis* is more complicated. It is smaller than *P. typicum*, and represented by more specimens than *P. figueirasi*, including a skull and a partial lower jaw, with a complete upper and lower dentition (Perea, 1988), as well as a second edentulous but slightly more complete lower jaw of similar age from Argentina, if one accepts the synonomy of *Senetia mirabilis* (Kraglievich,

1925; Riggs & Patterson, 1939; Brandoni, 2013) with this new material. It might be noted here that Riggs and Patterson (1939) initially assigned their fossils to *P. mirabilis* based on their resemblance to Kraglievich's (1925) specimen. Lastly, there are recognizable morphological distinctions between *P. mirabilis* and *P. typicum*, most notably the derived presence of a single pair of enlarged postpalatal foramina in the former and the derived elongation of the postpalatal shelf in the latter. That being said, the descriptions above note several instances of substantial morphological variation within *P. typicum* (*e.g.*, in the morphology of the basicranial surface and the shape of the upper and lower molariforms), and sloth skulls in general often show marked intraspecific variation (*e.g.*, Stock, 1925; Billet *et al.*, 2012; McAfee & Naples, 2012; De Iuliis *et al.*, 2014; Hautier *et al.*, 2014; Boscaini *et al.*, 2018a; De Iuliis, 2018). Therefore, although we tentatively accept the validity of *P. mirabilis,* we believe that more specimens and more detailed analyses are needed to confirm this taxonomic hypothesis.

We did not wish to undertake yet another phylogenetic analysis of relationships among nothrotheriid sloths as part of the present study. This is in part because this study represents a precursor to a more extensive study of the postcranial skeletal anatomy of *P. typicum*, and we feel a phylogeny should wait for its completion. We also prefer to wait because we are unsure whether a circumscribed study focused only on nothrotheriids is the best path forward. As noted in the introduction above, several such studies have been published in the past few decades, and these studies have failed to reach a consensus, particularly in regards to the position of the genera *Pronothrotherium* and *Mionothropus* relative to one another, and to the well-known Pleistocene Nothrotheriini (*i.e.*, *Nothrotherium* and *Nothrotheriops*). The patterns of resemblance evident in this skull description are complex. *Pronothrotherium* retains a number of plesiomorphic features (*i.e.*, shared resemblances with the basal megatherioid *Hapalops*) not observed in other nothrotheriids, such as a narrow palate, rectangular outline of Mf1, parietal eminence, temporal lines that merge with the nuchal crest, a rugose postglenoid region, and small paracondylar process. However, it also shares plesiomorphies with *Mionothropus*, including retention of a small caniniform tooth, a prominent buccinator fossa, a small lacrimal, strong temporal lines, a slender mandibular horizontal ramus, and processes of the mandibular ascending ramus that are equidistant from one another. As noted by De Iuliis *et al.* (2011), there are apomorphies linking *Pronothrotherium* to Nothrotheriini exclusive of *Mionothropus*, apomorphies linking *Mionothropus* to Nothrotheriini exclusive of *Pronothrotherium*, and apomorphies shared by *Pronothrotherium* and *Mionothropus* exclusive of Nothrotheriini. Additional examples of each are to be found in the descriptions of the present study – *e.g.*, the v-shaped maxillopalatine suture in *Pronothrotherium* and Nothrotheriini, a broad palate between the tooth rows in *Mionothropus* and Nothrotheriini, and a raised dorsal supraoccipital exposure and straight vomerine keel in *Pronothrotherium* and *Mionothropus*. Given the complexity of these resemblances, we feel that the best way to resolve these relationships is likely in a more comprehensive analysis of sloth relationships, including novel information garnered from new taxa or better preserved examples of previously known taxa, as in the recent analyses by Varela *et al.* (2019) and Boscaini *et al.* (2019), but also including new characters, especially from the postcranial skeleton, which are outnumbered by craniodental characters 3 to 1 or more in both studies. It is our hope that this study, and our ongoing analyses of the postcranial anatomy of *Pronothrotherium typicum*, can contribute significantly to new phylogenetic analyses and better phylogenetic resolution among living and extinct sloths.

CONCLUSION

The present study provides the first detailed descriptions and illustrations of the skull of the late Miocene–early Pliocene nothrotheriid sloth species *Pronothrotherium typicum,* based on well-preserved, nearly complete specimens from The Field Museum of Chicago. The skull of this taxon exhibits a number of unusual features, in particular those related to the remarkable vomerine extension in the roof of the nasopharynx and its extraordinary ventral keel. The skull also shows a complex pattern of primitive and derived resemblances to other well-known nothrotheriid taxa. As a consequence, more comprehensive phylogenetic analyses will be required to resolve its evolutionary relationships.

From a taxonomic standpoint, the present study tentatively confirms the presence of two species in

Pronothrotherium, P. mirabilis, known from the Huayquerian SALMA of Uruguay and Argentina, and *P. typicum*, an Argentine species with a much longer temporal range, extending from the Huayquerian to the Chapadmalalan SALMA. However, we do not accept the validity of a third proposed species, *P. figueirasi,* considering it instead a junior synonym of *P. mirabilis*.

ACKNOWLEDGMENTS

For access to specimens used in the present study, we thank B. Simpson, J. Flynn, and K. Angielczyk (FMNH); C. Shaw and A. Farrell, (LACMHC); and A. Kramarz and J. C. Fernicola (MACN). We thank A. Neander (University of Chicago) for her assistance with the CT-scanning, and J. Morgan Scott (University of Tennessee at Chattanooga) for her ever-excellent work in preparing the drawings for this paper. Lastly, we thank editor M. S. Bargo and two anonymous reviewers for their comments on earlier drafts of this manscript, which greatly improved the quality of the final paper. The work of TJG and AB was supported in part by the University of Tennessee at Chattanooga, including a sabbatical grant, the Freeman Award, and the Bramblett gift fund; the work of FP and AB, including the funding for CT scanning, was supported by a grant from the National Geographic Society (NGS 9971-16).

REFERENCES

Ameghino, F. (1907). Notas sobre una pequeña colección de huesos de mamíferos procedentes de las grutas calcáreas de Iporanga en el estado de São Paulo, Brazil. *Revista do Museu Paulista*, *7*, 59–124.

Amson, E., Muizon, C. de, & Gaudin, T. J. (2017). A reappraisal of the phylogeny of the Megatheria (Mammalia, Tardigrada), with an emphasis on the relationships of the Thalassocninae, the marine sloths. *Zoological Journal of the Linnean Society*, *179*, 217–236.

Bargo, M. S., De Iuliis, G., & Toledo, N. (2019). Early Miocene sloths (Xenarthra, Folivora) from the Río Santa Cruz valley (Southern Patagonia, Argentina). Ameghino, 1887 revisited. *Publicación Electrónica de la Asociación Paleontológica Argentina*, *19*, 102–137.

Bargo, M. S., Vizcaíno, S. F., & Kay, R. F. (2009). Predominance of orthal masticatory movements in the Early Miocene *Eucholaeops* (Mammalia, Xenarthra, Tardigrada, Megalonychidae) and other megatherioid sloths. *Journal of Vertebrate Paleontology*, *29*, 870–880.

Billet, G., Hautier, L., Asher, R. J., Schwarz, C., Crumpton, N., Martin, T., & Ruf, I. (2012). High morphological variation of vestibular system accompanies slow and infrequent locomotion in three-toed sloths. *Proceedings of the Royal Society B*, *279*, 3932–3939.

Bonini, R. A., Georgieff, S. M., & Candela, A. M. (2017). Stratigraphy, geochronology, and paleoenvironments of Miocene–Pliocene boundary of San Fernando, Belén (Catamarca, northwest of Argentina). *Journal of South American Earth Sciences*, *79*, 459–471.

Boscaini, A., Gaudin, T. J., Mamani-Quispe, B., Münch, P., Antoine, P.-O., & Pujos, F. (2018a). New well-preserved craniodental remains of *Simomylodon uccasamamensis* (Xenarthra, Mylodontidae) from the Pliocene of the Bolivian Altiplano: phylogenetic, chronostratigraphic, and paleobiogeographical implications. *Zoological Journal of the Linnean Society*, *185*, 459–486.

Boscaini, A., Iurino, D. A., Billet, G., Hautier, L., Sardella, R., Tirao, G., Gaudin, T. J., & Pujos, F. (2018b). Phylogenetic and functional implications of the ear region anatomy of *Glossotherium robustum* (Xenarthra, Mylodontidae) from the late Pleistocene of Argentina. *The Science of Nature [Naturwissenschaften]*, *105*, 28. https://doi.org/ 10.1007/s00114-018-1548-y

Boscaini, A., Iurino, D. A., Mamani Quispe, B., Andrade Flores, R., Sardella, R., Pujos, F., & Gaudin, T. J. (2020a). Cranial anatomy and paleoneurology of the extinct sloth *Catonyx tarijensis* (Xenarthra, Mylodontidae) from the late Pleistocene of Oruro, Southwestern Bolivia. *Frontiers in Ecology and Evolution*, *8*, 1–16.

Boscaini, A., Iurino, D. A., Sardella, R., Tirao, G., Gaudin, T. J., & Pujos, F. (2020b). Digital cranial endocasts of the extinct sloth *Glossotherium robustum* (Xenarthra, Mylodontidae) from the late Pleistocene of Argentina: description and comparison with the extant sloths. *Journal of Mammalian Evolution*, *27*, 55–71.

Boscaini, A., Pujos, F., & Gaudin, T. J. (2019). A reappraisal of the phylogeny of Mylodontidae (Mammalia, Xenarthra) and the divergence of mylodontine and lestodontine sloths. *Zoologica Scripta*, *48*, 691–710.

Brandoni, D. (2013). Los Tardigrada (Mammalia, Xenarthra) del Mioceno tardío de Entre Ríos, Argentina. In D. Brandoni and J. I. Noriega (Eds.), *El Neógeno de la Mesopotamia argentina. Asociación Paleontológica Argentina, Publicación Especial 14*, 135–144.

Brandoni, D., & McDonald, H. G. (2015). An enigmatic Nothrotheriinae (Xenarthra, Tardigrada) from the Pleistocene of Argentina. *Ameghiniana*, *52*, 294–302.

Brandoni, D., & Vezzosi, R. I. (2019). *Nothrotheriops* sp. (Mammalia, Xenarthra) from the Late Pleistocene of Argentina: implications for the dispersion of ground sloths during the Great American Biotic Interchange. *Boreas*, *48*, 879–890.

Burmeister, G. (1882). *Nothropus priscus*, ein bisher unbekanntes fossiles Faulthier. *Sitzungsberichte der (Königlich-preussischen) Akademie der Wissenschaftenzu, Berlin, 1882*, 613–620.

Cartelle, C. (2012). *Das Grutas À Luz: Os Mamíferos Pleistocênicos de Minas Gerais*. Belo Horizonte, Brazil: Bicho do Mato Editora, 1ª edição.

Cartelle, C., & Fonseca J. S. (1983). Contribuição ao melhor conhecimento da pequena preguiça terrícola *Nothrotherium maquinense* (Lund) Lydekker, 1989. *Lundiana*, *2*, 127–181.

Cartelle, C., & Bohórquez, G. A. (1986). Descrição das pré-maxilas de *Nothrotherium maquinense* (Lund) Lydekker, 1889 (Edentata, Megalonychidae) e de *Eremotherium laurillardi* (Lund) Cartelle et Bohórquez, 1982 (Edentata, Megatheriidae). *Iheringia Séries Geológica*, *11*, 9–14.

De Iuliis, G. (1994). Relationships of the Megatheriidae, Nothrotheriinae and Planopsinae: some skeletal characteristics and their importance for phylogeny. *Journal of Vertebrate Paleontology*, *14*, 577–591.

De Iuliis, G. (2018). Recent progress and future prospects in fossil xenarthran studies, with emphasis on current methodology in sloth taxonomy. *Journal of Mammalian Evolution*, *25*, 449–458.

De Iuliis, G., Gaudin, T. J., & Vicars, M. P. (2011). A new genus and species of nothrotheriid sloth (Xenarthra, Tardigrada, Nothrotheriidae) from the late Miocene (Huayquerian) of Peru. *Palaeontology*, *54*, 171–205.

De Iuliis, G., McDonald, H. G., Stanchly, N., Spenard, J., & Powis, T. G. (2015). *Nothrotheriops shastensis* (Sinclair) from Actun Lak: first record of Nothrotheriidae (Mammalia, Xenarthra, Pilosa) from Belize. *Ameghiniana*, *52*, 153–171.

De Iuliis, G., Pujos, F., Toledo, N., Bargo, M. S., & Vizcaíno, S. F. (2014). *Eucholoeops* Ameghino, 1887 (Xenarthra, Tardigrada, Megalonychidae) from the Santa Cruz Formation, Argentine Patagonia: implications for the systematics of Santacrucian sloths. *Geodiversitas*, *36*, 209–255.

Delsuc, F., Kuch, M., Gibb, G. C., Karpinski, E., Hackenberger, D., Szpak, P., Martínez, J. G., Mead, J. I., McDonald, H. G., MacPhee, R. D. E., Billet, G., Hautier, L., & Poinar, H. N. (2019). Ancient mitogenomes reveal the evolutionary history and biogeography of sloths. *Current Biology*, *29*, 1–12.

Edmund, G. (1985). The fossil giant armadillos of North America (Pampatheriinae, Xenarthra = Edentata). In G. G. Montgomery (Ed.), *The Ecology and Evolution of Armadillos, Sloths, and Vermilinguas* (pp. 83–93). Smithsonian Institution Press, Washington, D.C.

Engelmann, G. (1985). The phylogeny of the Xenarthra. In G. G. Montgomery (Ed.), *The Ecology and Evolution of Armadillos, Sloths, and Vermilinguas* (pp. 51–64). Smithsonian Institution Press, Washington, D.C.

Esteban, G., Nasif, N., & Georgieff, S. (2014). Cronobioestratigrafía del Mioceno tardío–Plioceno temprano, Puerta de Corral Quemado y Villavil, Provincia de Catamarca, Argentina. *Acta Geologica Lilloana*, *26*, 165–192.

Evans, H. E., & Christensen G. C. (1979). *Miller's Anatomy of the Dog*. W.B. Saunders Co., Philadelphia.

Ferigolo, J. (1985). Evolutionary trends of the histological pattern in the teeth of Edentata (Xenarthra). *Archives of Oral Biology*, *30*, 71–82.

Frailey, C. D. (1986). Late Miocene and Holocene mammals, exclusive of the Notoungulata, of the Río Acre region, western Amazonia. *Contributions in Science, Natural History Museum of Los Angeles County*, *374*, 1–74.

Gaudin, T. J. (1995). The ear region of edentates and the phylogeny of the Tardigrada (Mammalia, Xenarthra). *Journal of Vertebrate Paleontology*, *15*, 672–705.

Gaudin, T. J. (2004). Phylogenetic relationships among sloths (Mammalia, Xenarthra, Tardigrada): the craniodental evidence. *Zoological Journal of the Linnean Society*, *140*, 255–305.

Gaudin, T. J. (2011). On the osteology of the auditory region and orbital wall in the extinct West Indian sloth genus *Neocnus* (Megalonychidae, Xenarthra, Placentalia). *Annals of the Carnegie Museum of Natural History*, *80*, 5–28.

Gaudin, T. J., De Iuliis, G., Toledo, N., & Pujos, F. (2015). The basicranium and orbital region of the early Miocene *Eucholoeops ingens* Ameghino, 1887 (Xenarthra, Pilosa, Megalonychidae). *Ameghiniana*, *52*, 226–240.

Gaudin, T. J., & Lyon, L. M. (2017). Cranial osteology of the pampathere *Holmesina floridanus* (Xenarthra: Cingulata; Blancan NALMA), including a description of an isolated petrosal bone. *PeerJ, 5*, e4022, 73 pp. DOI 10.7717/peerj.4022

Gaudin, T. J., Wible, J. R., Hopson, J. A., & Turnbull, W. D. (1996). Reexamination of the morphological evidence for the Cohort Epitheria (Mammalia, Eutheria). *Journal of Mammalian Evolution*, *3*, 31–79.

Guth, C. (1961). *La région temporale des Édentés.* [Ph. D. Dissertation, Université de Paris, Paris].

Hautier, L., Billet, G., Eastwood, B., & Lane, J. (2014). Patterns of morphological variation of extant sloth skulls and their implication for future conservation efforts. *The Anatomical Record*, *297*, 979–1008.

Kalthoff, D. C. (2011). Microstructure of dental hard tissues in fossil and recent xenarthrans (Mammalia: Folivora and Cingulata). *Journal of Morphology*, *272*, 641–661.

Kraglievich, L. (1925). Un nuevo eslabón en la serie filogenética de la subfamilia Nothrotheriinae: *Senetia mirabilis. Anales del Museo de Historia Natural de Buenos Aires*, *33*, 177–193.

Kraglievich, L. (1926). Presencia del género "*Nothrotherium*" Lydek. (= "*Coelodon*" Lund) en la fauna pampeana "*Nothrotherium torresi*", n. sp. *Revista del Museo de La Plata*, *29*, 169–186.

Lull, R. S. (1929). A remarkable ground sloth. *Memoirs of the Peabody Museum of Yale University*, *3*, 1–39.

Marshall, L. G., & Patterson, B. (1981). Geology and geochronology of the mammal-bearing Tertiary of the Valle de Santa María and Río Corral Quemado, Catamarca Province, Argentina. *Fieldiana Geology*, *9*, 1–80.

McAfee, R. K., & Naples, V. L. (2012). Notice on the occurrence of supernumerary teeth in the two-toed sloths *Choloepus didactylus* and *C. hoffmanni. Mastozoología Neotropical*, *19*, 339–344.

McDonald, H. G., & De Iuliis, G. (2008). Fossil history of sloths. In S. F. Vizcaíno, & W. J. Loughry (Eds.), *The Biology of the Xenarthra* (pp. 39–55). Gainesville, University of Florida Press, Gainesville.

McDonald, H. G., & Muizon, C. de (2002). The cranial anatomy of *Thalassocnus* (Xenarthra, Mammalia), a derived nothrothere from the Neocene of the Pisco Formation (Peru). *Journal of Vertebrate Paleontology*, *22*, 349–365.

Muizon, C. de, & McDonald, H. G. (1995). An aquatic sloth from the Pliocene of Peru. *Nature*, *375*, 224–227.

Muizon, C. de, McDonald, H. G., Salas, R., & Urbina, M. (2003). A new early species of the aquatic sloth *Thalassocnus* (Mammalia, Xenarthra) from the late Miocene of Peru. *Journal of Vertebrate Paleontology*, *23*, 886–894.

Muizon, C. de, McDonald, H. G., Salas, R., & Urbina, M. (2004). The youngest species of the aquatic sloth *Thalassocnus* and a reassessment of the relationships of the nothrothere sloths (Mammalia: Xenarthra). *Journal of Vertebrate Paleontology*, *24*, 387–397.

Naples, V. L. (1985). Form and function of the masticatory musculature in the tree sloths, *Bradypus* and *Choloepus*. *Journal of Morphology*, *183*, 25–50.

Naples, V. L. (1990). Morphological changes in the facial region and a model of dental growth and wear pattern development in *Nothrotheriops shastensis*. *Journal of Vertebrate Paleontology*, *10*, 372–389.

Naples, V. L., & McAfee, R. K. (2014). Chewing through the Miocene: an examination of the feeding musculature in the ground sloth *Hapalops* from South America (Mammalia: Pilosa). *F1000Research*, *3*, 86. https://doi: 10.12688/f1000research.3282.1. eCollection 2014

Owen, R. (1856). On the *Megatherium* (*Megatherium americanum*, Cuvier and Blumenbach). Part III. The skull. *Philosophical Transactions of the Royal Society of London*, *146*, 571–589.

Patterson, B., Segall, W., Turnbull, W. D., & Gaudin, T. J. (1992). The ear region in xenarthrans (= Edentata, Mammalia). Part II. Pilosa (sloths, anteaters), palaeanodonts, and a miscellany. *Fieldiana, Geology new series*, *24*, 1–79.

Paula Couto, C. de (1971). On two small Pleistocene ground sloths. *Anais da Academia Brasileira de Ciências*, *43*, 499–513.

Paula Couto, C. de (1979). *Tratado de Paleomastozoologia.* Academia Brasileira de Ciências, Rio de Janeiro.

Paula Couto, C. de (1980). Pleistocene mammals from Minas Gerais and Bahia, Brazil. *Actas II Congreso Argentino de Paleontología y Bioestratigrafía y I Congreso Latinoamericano de Paleontología*, *3*, 193–209.

Perea, D. (1988). Dos Nothrotheriinae (Tardigrada, Megatheriidae) del Mio–Plioceno de Uruguay. *Ameghiniana*, *25*, 381–388.

Perea, D. (1999). Un singular grupo de perezosos, los 'Nothrotheriinae' (Xenarthra). *Boletín de la Sociedad Zoologica de Uruguay*, *10*, 1–8.

Perea, D. (2007). *Nothrotherium* cf. *N. maquinense* (Xenarthra, Tardi-

grada) en la Formación Sopas (Pleistoceno tardío de Uruguay). *Revista de la Sociedad Uruguaya de Geología*, *14*, 5–9.

Pick, T. P., & Howden, R. (1977). *Gray's Anatomy, 15th ed.* Bounty Books, New York.

Presslee, S., Slater, G. J., Pujos, F., Forasiepi, A. M., Fischer, R., Molloy, K., Mackie, M., Olsen, J. V., Kramarz, A. G., Taglioretti, M., Scaglia, F., Lezcano, M., Lanata, J. L., Southon, J., Feranec, R., Bloch, J., Hajduk, A., Martin, F. M., Salas Gismondi, R., Reguero, M., Muizon de, C., Greenwood, A., Chait, B. T., Penkman, K., Collins, M., & MacPhee, R. D. E. (2019). Palaeoproteomics resolves sloth relationships. *Nature Ecology & Evolution*, *3*, 1121–1130.

Pujos, F., De Iuliis, G., & Cartelle, C. (2017). A paleogeographic overview of tropical fossil sloths: towards an understanding of the origin of extant suspensory sloths? *Journal of Mammalian Evolution*, *24*, 19–38.

Pujos, F., De Iuliis, G., Mamani Quispe, B., Adnet, S., Andrade Flores, R., Billet, G., Fernández-Monescillo, M., Marivaux, L., Münch, P., Prámparo, M. B., & Antoine, P.-O. (2016). A new nothrotheriid xenarthran from the early Pliocene of Pomata-Ayte (Bolivia): new insights into the caniniform–molariform transition in sloths. *Zoological Journal of the Linnean Society*, *178*, 679–712.

Pujos, F., De Iuliis, G., Mamani Quispe, B., & Andrade Flores, R. (2014). *Lakukullus anatirostratus*, gen. et sp. nov., a new massive nothrotheriid sloth (Xenarthra, Pilosa) from the middle Miocene of Bolivia. *Journal of Vertebrate Paleontology*, *34*, 1243–1248.

Reguero, M. A., & Candela, A. M. (2011). Late Cenozoic mammals from the northwest of Argentina. In J. A. Salfity, and R. A. Marquillas (Eds.), *Cenozoic Geology of the Central Andes of Argentina* (pp. 411–426). SCS Publisher, Salta.

Reinhardt, J. (1878). Kæmpedovendyr-Slægten *Coelodon*. *Danske Videnskabernes Selskab Skrifter, Naturvidenskabelig og Mathematisk Afdeling*, *12*, 255–349.

Riggs, E. S., & Patterson, B. (1939). Stratigraphy of late Miocene and Pliocene deposits of the Province of Catamarca (Argentina) with notes on the fauna. *Physis*, *14*, 143–162.

Rovereto, C. (1914). Los estratos araucanos y sus fósiles. *Anales del Museo Nacional de Buenos Aires*, *25*, 1–249.

Scott, W. B. (1903). Mammalia of the Santa Cruz Beds. Part 1. Edentata 2. Glyptodontia and Gravigrada. *Reports of the Princeton Expeditions to Patagonia*, *5*, 107–227.

Scott, W. B. (1904). Mammalia of the Santa Cruz Beds. Part 1. Edentata 3. Gravigrada. *Reports of the Princeton Expeditions to Patagonia*, *5*, 227–364.

Stock, C. (1925). Cenozoic gravigrade edentates of western North America, with special reference to the Pleistocene Megalonychidae and Mylodontidae of Rancho la Brea. *Carnegie Institution of Washington Publications*, *331*, 1–206.

Varela, L., Tambusso, P. S., McDonald, H. G., & Fariña, R. A. (2019). Phylogeny, macroevolutionary trends and historical biogeography of sloths: insights from a Bayesian morphological clock analysis. *Systematic Biology*, *68*, 204–218.

Wible, J. R., & Gaudin, T. J. (2004). On the cranial osteology of the yellow armadillo *Euphractus sexcinctus* (Dasypodidae, Xenarthra, Placentalia). *Annals of the Carnegie Museum of Natural History*, *73*, 117–196.

Wilson, R. W. (1942). Preliminary study of the fauna of Rampart Cave, Arizona. *Contributions to Paleontology, Carnegie Institution of Washington Publications*, *530*, 169–185.

Editorial Note: Both this work and the nomenclatural acts it contains have been registered in the ZooBank. The work is permanently archived in the Internet Archive.

LSID urn:lsid:zoobank.org:pub:8DAE418E-EBDC-477B-9920-8682F52B170C

doi: 10.5710/PEAPA.04.09.2020.320

Recibido: 5 de junio 2020
Aceptado: 4 de septiembre 2020
Publicado: 17 de noviembre 2020